Using geophysical subsurface data for the reconstruction of valley-scale spatio-temporal floodplain evolution: Implications for upland river restoration.

Arved C. Schwendel[1], David J. Milan[2], Richard J.J. Pope[3], Richard Williams[4] and Warren Thompson[5]

[1]School of Humanities, York St John University, York, YO31 7EX, UK; a.schwendel@yorksj.ac.uk

[2]School of Environmental Sciences, University of Hull, Hull, UK

[3]Department of Environmental Sciences, School of the Built and Natural Environment, University of Derby, Derby, DE22 1GB, UK

[4]School of Geographical and Earth Sciences, University of Glasgow, Glasgow, G12 8QQ, UK

[5]Department of Physics, Technical University of Denmark, Risø Campus, DK- 4000 Roskilde, Denmark.

Abstract

The use of analogues of previous river styles is highly significant for successful river restoration, yet some existing techniques available to assist practitioners are still not widely applied. We explore the use of Ground Penetrating Radar (GPR), to explore past river styles in an upland river valley in the UK, and explore the potential of the approach to reconstruct former channel pattern. Post-glacial evolution of upland floodplains has been influenced by temporal changes in vegetation, sediment supply and hydrological regime. Channel-floodplain morphodynamics over the Holocene were conditioned by glacial deposits, lateral interaction with slope processes and fluvial sediment reworking, changes in flow and sediment supply regimes driven by climatic change, and more recently direct and indirect anthropogenic activities, e.g. deforestation, floodplain land use and channel modification. Current drives towards river restoration, often use floodplain topography as a guide to appraise such a planform state, however, reconstruction of former channel state is often restricted to surface features visible on historic maps and aerial photographs. This research focuses upon the floodplain of the upper Swindale Beck, Lake District, UK, which was recently restored to a planform design based on the recent meander pattern visible in floodplain topography. We show the potential of GPR to reconstruct a wider array of past channel pattern and evolution at a site characterised by largely aggradational conditions and consistent sediment supply from glacial deposits at the valley head. Analysis of GPR data from 40 intersecting GPR survey lines revealed several stratigraphic units, including gravel braidplains, berms, chutes and bars, several levels of larger channels and their layered fill as well as backwater deposits. These were interpreted as braided systems, dynamic wandering planform and single-thread meandering systems with spatial transitions conditioned by tributaries and valley slope. Optically Stimulated Luminescence (OSL) dates in combination with GIS analysis of valley slope, channel gradient and local valley floor aspect allowed the interpretation of individual evolutionary stages of river and floodplain development at Swindale over at least the last millennium and provides links to processes in the wider environment including the role of alluvial fans in supplying sediment and forcing channel migration. Such information can be particularly valuable for restoration projects to aid design of channel dimensions, planform configuration, channel gradient, substrate characteristics and connection with tributaries. While restoration generally aims to resemble a more natural reference state, specific targets may seek to improve a particular set of functionalities (e.g., ecological, flood and sediment management, recreational) which should be resilient to the consequences of ongoing climatic changes and should be achieved sustainably (e.g. locally sourced gravel). Here, GPR-based floodplain analysis provides a non-invasive approach to understand possible evolutionary trajectories and to appraise a wider range of restoration options and sustainable resources.

Keywords

Ground Penetrating Radar; Alluvial stratigraphy; Paleochannel reconstruction; River realignment; Geomorphological tools; Optically Stimulated Luminescence Dating

1. Introduction

River restoration design and construction predominantly focuses upon considerations of planform pattern and channel three-dimensional shape. Initial efforts at river manipulation for aesthetic and recreational purposes has been conducted for over a century (Wohl et al., 2015; Podolak and Kondolf, 2016), with creation of single-thread channels with riparian woodland (Kondolf, 2006) and introduction of instream structures to improve trout fishing e.g., in the US (Van Cleef, 1885; Hubbs et al., 1932; Thompson and Stull, 2002). During the 1980s river restoration primarily concentrated on fish habitat improvements (e.g., Gowan and Fausch, 1996), which involved introduction of plants, dead wood or morphological modification (Wohl et al., 2015). There has been an intensification in river re-naturalisation and restoration over the last three decades, in an attempt to restore physical and ecological functioning. In Europe, this in part has been driven by European legislation (EU Water and Habitats directives), and more recently in the UK through Natural Flood Management. During this period there has been an increasing realisation that successful restoration needs to be informed through geomorphological, hydrological and ecological concepts, requiring an interdisciplinary and catchment-scale approach (Harper et al., 1999; Sear, 1994). River restoration is a form of management that seeks to improve hydrologic, geomorphic and ecological processes (Wohl et al., 2005), however, often the design includes additional functionality and targets such as natural flood management, sediment management, habitat quality, ecological diversity or recreational and aesthetic considerations (Wohl et al., 2015). It is increasingly thought that restoring full functionality to river systems is a way forward, using both hydrological and geomorphological knowledge and principles, to improve channel dynamism through reinstating former channel form (e.g., Newson and Large, 2006; Sear, 1994; Soar et al., 1998; Walker et al., 2007). This often allows other targets to be met, such as improving floodplain connectivity, hydraulic diversity, water quality and sediment transport, thus often leading to improved habitat condition.

Although the problems within fluvial systems are often catchment-wide, river restoration has tended to focus on ad-hoc reach-scale efforts, often addressing the most severely degraded sections of river e.g., channelised areas (Harper et al., 1999). Current river restoration projects are wide-ranging, and may involve channel redesign (Prior, 2016), usually informed by past channel styles, including restoration to a meandering planform (Kondolf, 2006), anabranching (Medel et al., 2022), or braided channels (Brousse et al., 2021). Other projects have included reconnection of the channel with the floodplain recreating wetlands (Tockner et al., 1999; Gumiero et al., 2013), replanting forest in upland areas (to increase interception and evapotranspiration) and on floodplains to increase hydraulic roughness (Harper et al., 1999; Antonarakis and Milan, 2020), introducing large wood to rivers systems (Grabowski et al., 2019), re-introducing beavers (Curran et al., 2014), removing dams and weirs to improve longitudinal connectivity (Sneddon et al., 2017; Garcia de Leaniz, 2008), gravel augmentation (Milan et al., 2000; Arnaud et al., 2017), blocking artificial drainage systems e.g. upland grips (Ramchunder et al., 2012), consideration of hyporheic function (Hester and Gooseff, 2011), and more recently ‘stage zero’ approaches (Powers et al., 2019). All of these are informed to varying degrees by geomorphological, hydrological and ecological understanding and concepts.

Reach-scale channel restoration is often focused upon diversifying hydraulic habitat, and reintroducing such features as pool-riffle morphology, barforms and spawning gravels for fish, and reconnecting the channel to the floodplain. Usually there is an attempt to recreate the channel morphology prior to the channel being engineered. Often the challenge to the river restoration practitioner is defining a reference state, and the channel morphology that should be restored (Newson and Large, 2006). The solution is not aways straightforward. Many early river restoration designs arguably were strongly steered towards the public perception view of what an ideal river should look like; usually single-thread meandering (e.g. Prior, 2016), which for the UK at least we now know this not necessarily to be the case (Lewin, 2010). However, river morphodynamics and planform configuration respond to changes in climate and land use and as such sustainable river management needs to incorporate planning for anticipated future changes (Church and Ferguson, 2015). Intense precipitation has increased globally in the 20th century and is predicted to become more frequent in future, across many places (Groisman et al., 2005; Beniston, 2009). In the UK there is some evidence for increased flood magnitudes that may be associated with this climate change (Wilby et al., 2008; Hannaford and Buys, 2012; Dadson et al., 2017). The consequences for river systems are not only frequent extreme floods and related sediment fluxes, but also the reduced potential of river reaches to recover (e.g., maintain their previous planform configuration) from such events (Milan and Schwendel, 2021).

A number of studies advocate the use of fluvial audit approaches (Sear et al., 1995; Sear et al., 2009) to guide the practitioner towards sustainable approaches to river restoration. This usually will include a historical assessment of former channel pattern using historic aerial images, maps and LiDAR data to reconstruct former channel pattern and planform morphology (e.g. Sear, 1994). However, the use of analogues of past river styles tends to be underused or sometimes ignored, partly due to the target of the river restoration but also due to the limited information or technology available. Although there have been recent advances in the availability and application of remote sensing data for fluvial environments including its use in river restoration (Entwistle et al., 2018), far less attention has been paid to the potential of subterranean information for river restoration.

Despite repeated calls for a more process-based approach to river restoration (Beechie et al., 2010), it is relatively uncommon for an understanding of sub-surface sedimentology and stratigraphy to be used in river restoration but it has twofold potential. First, assessment of valley floor stratigraphy can give insight into past river and floodplain configuration, and associated evolutionary histories. However, simply attempting to create the previous channel morphologies, that functioned under a different hydrological and sediment supply regime, controlled by past climatic conditions and land-use, is not always a sustainable solution. Hence any re-designed channel must not only be based on contextual understanding of past channel form, but must also take into consideration of contemporary and future trajectories in environmental forcing conditions. The utilisation of geophysical approaches coupled with dating methodologies have potential to address this gap and to shed light on the likely trajectory of past channel form development and suitability as a target for design (Słowik, 2015). Second, when process-based restoration is designed to give a river space to move (Biron et al., 2014; Piégay et al., 2005) and a river is expected to scour its bed and erode its banks (Williams et al., 2020) to adjust to variations in water and sediment discharge, understanding of sub-surface sedimentology can give insight into how vertical hydrologic connectivity may change (Sparacino et al., 2019; Howard et al., 2024) and the calibre of material that may be entrained and transported downstream. The primary methodological approach to map subsurface sedimentology is Ground Penetrating Radar (GPR). Its application in river restoration is uncommon but there are examples where surface GPR has been used to inform on past channel patterns as a basis for restoration (e.g. Słowik, 2015), identify boundaries in sediment stratigraphy (Schneider et al., 2011), for the estimation of fine sediment depth and underlying coarse bedforms upstream of weirs using boat-based GPR (Schwendel, 2019) and borehole and surface GPR for the characterisation of gravel aquifers (Doetsch et al., 2010; 2012).

Here we argue that successful river restoration design can be informed by a full chronology of channel response over time. To achieve this, river restoration practitioners should have a variety of tools available at their disposal to make informed decisions. In this paper we explore the use of Ground Penetrating Radar (GPR), as an additional tool to the river restoration practitioner, to inform on historic channel pattern and evolution. The specific aims of our investigation were:

1) Reconstruction of stages of channel planform development and floodplain evolution based on GPR data in the context of local conditioning influences (e. g. alluvial fans, moraines);
2) Appraisal of the temporal scale of such development ;

3) Contextualisation of more recent anthropogenic alterations (straightening and realignment during restoration) with past river styles;
4) Evaluation of the benefits of GPR floodplain survey as a tool for river restoration practitioners.

2. Study site

2.1 Site context

The common channel morphology during the mid Holocene in the UK was multi-thread anastomosed (Brown and Keough, 1992). Human impacts upon UK rivers date back to the Bronze Age when human activity significantly altered this channel form and associated riparian forest, and with evidence of landscape-scale deforestation detectable in pollen record (Brown, 1997; Heritage et al., 2021). As farming practices improved through the Iron Age, tree felling became more widespread altering catchment-scale hydrology and sediment supply, with subsequent effects on channel and floodplain form and function. Low intensity farming existed alongside unconstrained rivers until the Middle Ages, after which channel modification became more common and significant areas of wetland were drained to increase productivity. Anastomosed channels possibly in fossilised form are thought to have been the dominant channel type up to late Medieval period (Lewin, 2010). Human impact accelerated after the 15th century, where rivers were impounded to provide water for agriculture and power (Bravard and Petts, 1996), and floodplains in the UK changed drastically (Lewin, 2013). By the 1900s rivers in industrial Britain had been extensively channelised, restricting movement and natural morphological development (Johnson, 1954). Modified straight channels often had levees along the bank tops, effectively disconnecting the channel from the floodplain. Over the 20th century, land drainage and flood relief saw further loss of natural river and floodplain form and function. More recently, post-World War 2 agricultural intensification saw artificial drainage systems installed in large areas of land in catchments, intensifying runoff of both water and sediment, and altering hydrograph shapes (Holden et al., 2006). Rapid urbanisation also influenced hydrograph character and sediment supply (Miller et al., 2017). As floodplain productivity increased and land values rose, these areas were protected from flooding by embanking, decreasing channel-floodplain connectivity, and increasing flood risk downstream.

2.2 Site description

The study site at Swindale is situated at 265 m a.s.l. on the eastern edge of the English Lake District in a glacial trough valley with a tributary hanging valley (Mosedale) and a cirque-shaped valley head (Evans and Cox, 1995; Wilson and Clark, 1998) approximately 800 m upstream (Fig. 1). Swindale Beck drains in a north-westerly direction to the River Lowther. The catchment upstream of the study site comprises 15.3 km^2 of acidic grasslands with heather and bracken in the uplands and improved grassland with patches of woodland in the valley. Late Ordovician volcanoclastic sandstones and breccia of the Borrowdale Volcanic Group are overlain by till, peat and alluvial deposits (Millward, 2003). Andesitic sills are cropping out in the channel downstream of the site (BGS, 2013) where a water intake is located, and provide a local base level, thus creating a largely aggradational setting at the site. The same sills appear as a roche moutonneé near the valley head (Wilson and Clark, 1998), where Swindale Beck, coming from the hanging valley of Mosedale, erodes into a cluster of Younger Dryas moraines (Lunn, 1990; Wilson and Clark, 1998; Bickerdike et al., 2016) (Fig. 2). McDougall (2013) suggests the possibility that glaciation extending from summit icefields could have extended further down-valley across the study site during this stadial and indicates associated moraines (Fig. 1c). Other geomorphological features in the valley include talus cones and alluvial fans associated with high gradient tributaries (BGS, 2013) (Fig. 2).

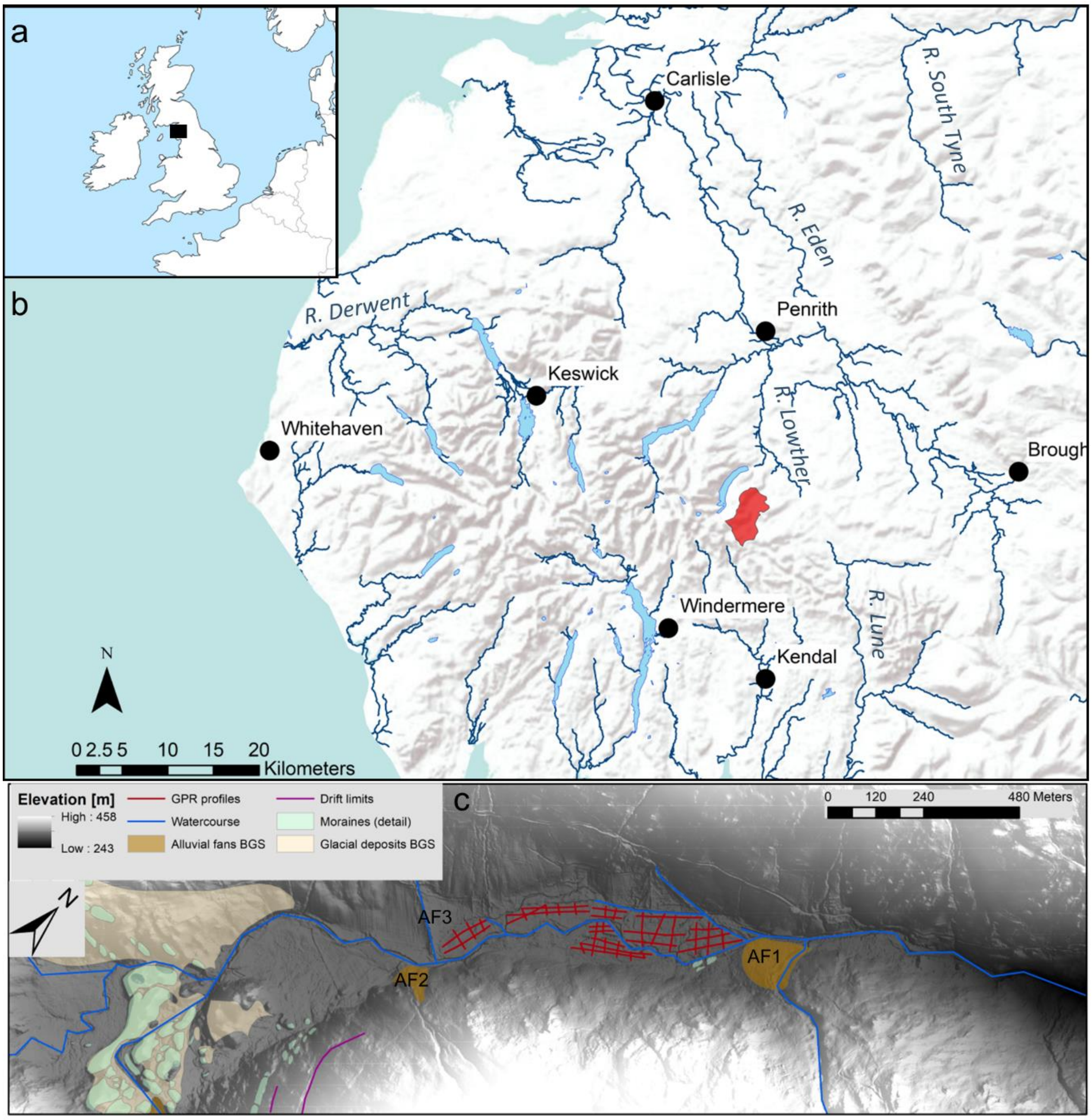

Figure 1. Location of the study site a) within British Isles (data source: Natural Earth) and b) the English Lake District. The catchment at the downstream end of the study site is shaded in red (data sources: CEH, ESRI, Natural Earth). Panel c) shows a 2020 lidar DTM of the glacial trough valley of Swindale with the study site indicated by GPR profiles (Data source: National Lidar Programme, 2021, Open Government Licence). Valley confinement due to bedrock outcrops is visible downstream of the site. Glacial deposits, as mapped by the British Geological Survey (BGS, 2013) and in detail by Bickerdike et al. (2016), and alluvial fans (AF) provide sediment and lateral constraint.

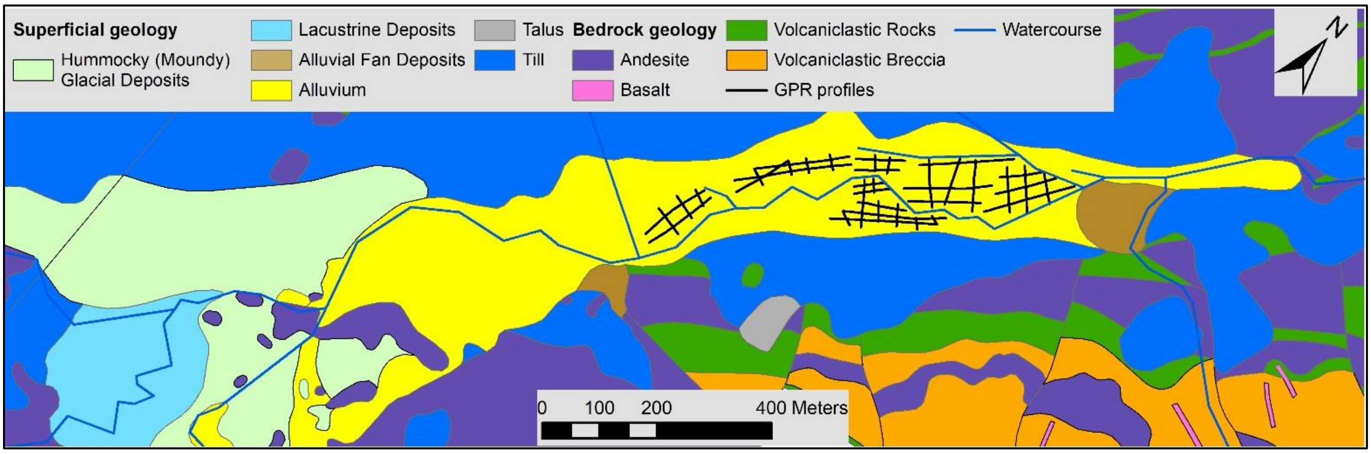

Figure 2. Geology of Swindale (Data source: DiGMapGB-10, 1:10000 using EDINA Geology Digimap Service). The studied area is indicated by GPR profiles. Andesite outcrops in the valley downstream of the study site (shown by the location of GPR profiles) provide base level control for floodplain evolution.

At the study site the channel had been straightened prior to the first edition of the Ordnance Survey map for this area (surveyed 1858 to 1859, published 1863) for improved agricultural use of the floodplain with the latter also being drained. The banks of the straightened channel were protected by a boulder toe in places (Reid, 2015). The substrate was dominated by cobbles with some gravel with median grain size ranging from 82 mm upstream to 133 mm downstream (Reid, 2015). In 2016 a United Utilities and RSPB led two-phase restoration scheme was implemented that aimed to improve river habitat quality and wildlife recovery while maintaining farm operations (hay meadows) on the floodplain (Wightman and Schofield, 2021). The design of Phase 1 was guided by palaeochannel mapping, channel coring to determine the existence and elevation of gravel deposits, interpretation of floodplain elevations to determine flowpaths across the floodplain, and involved designing channels using hydraulic geometry principles. The Phase 1 restoration realigned a previously straight, incised channel to a meandering planform, guided by the sinuosity observed in well-defined palaeochannels on the floodplain in the downstream segment of the study site. Phase 2 involved remeandering the upstream segment of the scheme. Compared to Phase 1, the scheme design had a lower sinuosity. The phases were joined where the Beck was previously straight. The former straight channel was in most places backfilled with spoil from excavation of the new channel (Fig. 3). The scheme is part of a broader set of nature-based catchment management approaches that have been implemented throughout the catchment (Hankin et al., 2019). The floodplain is largely flat with some partially infilled channels of lower width than the current single-thread channel. It was used at the time of investigation as a hay meadow. The study site forms part of the Site of Special Scientific Interest (SSSI) Swindale Meadows and is designated a Special Area for Conservation.

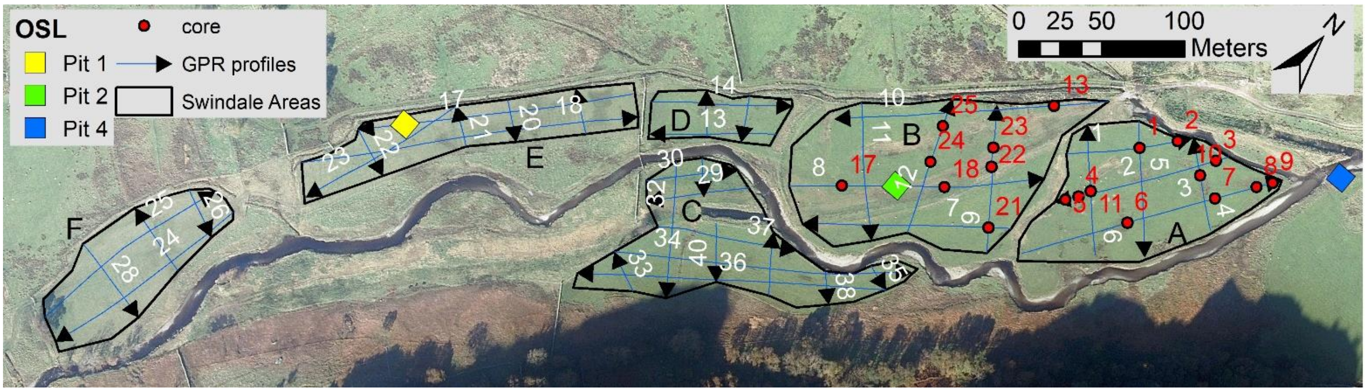

Figure 3. Detailed location of GPR profiles, OSL samples and cores in Swindale. The survey was carried out in 6 areas (A to F) separated by the current channel of Swindale Beck, dry stone walls or deep palaeochannels that could not be traversed by the GPR cart. The river channel has been realigned in 2016 but the course of the former straight channel can still be seen as a faint pattern in the grass east of areas E and F and traversing areas C and B (see also facies VI in Fig. 5d). High resolution (25 cm) vertical aerial imagery from 2018 has been sourced from Getmapping using EDINA Aerial Digimap Service.

3. Methods

3.1 Ground Penetrating Radar and coring

At Swindale the floodplain stratigraphy was explored in July 2018 with Ground Penetrating Radar (GPR) at 40 intersecting survey lines (Fig. 3) with a total length of 3283 m, covering an area of approximately 5.1 ha. The grassland had been recently mown apart from deep depressions which were not surveyed across. A PulseEkko Pro GPR (Sensors&Software, Mississauga, Canada) with a 100 MHz antenna and constant separation of 1 m from the receiver was used in reflection mode (time window 200 ns, step size: 0.25 m, 250 samples per trace and a stack height of 32). These settings are suitable for investigations in floodplains with potentially conductive soil (Vandenberghe and van Overmeeren, 1999; Słowik, 2012b) and have been successfully applied in similar settings (e.g. Bridge et al., 1995; Gourry et al., 2003; Kostic and Aigner, 2007; Hickin et al., 2009; Dara et al., 2019; Słowik et al., 2021; Elznicová et al., 2023). Signal velocity was assessed from diffraction hyperbolas at several profiles and depths. As the identified velocities were similar across profiles and depths a mean value of 0.075 m/ns was subsequently adopted for all profiles for consistency. This allows a nominal vertical resolution (separation between two reflectors) of approximately 0.19 m (Neal, 2004). Depth penetration of the radar signal was limited by material of high electric conductivity at a depth of 1.5 – 4 m which is most likely associated with glacial deposits.

The start, end and some intermediate points of each profile were recorded in the field with a Leica 1200 dGNSS system (Leica Geosystems, Heersbrugg, Switzerland). Surface topography was measured in a GIS (ArcMap 10.5.1, ESRI, Redlands, USA) from a publicly available 1-m aerial lidar DTM from 2021 (Environment Agency, UK).

GPR data processing was carried out in ReflexW 9.1 (Sandmeier, Karlsruhe, Germany) and involved Devow, background subtraction, application of an exponential gain function and topographic correction (Neal, 2004). Further processing such as bandpass filtering or dynamic correction did not result in improved radargrams and was therefore not used. Some profiles benefitted from the application of the calculation of instantaneous amplitudes (envelope filter) in order to simplify reflections and to show their true resolution.

After preliminary analysis, 19 locations for ground truthing (Fig. 3) were selected and cored up to a maximal depth of 2.1 m using an Eijkelkamp hand auger. The depth of coring was limited by the presence of coarse layers that were either impenetrable or caused collapse of the bore hole. Additional information was derived from cutbank exposures of the new river channel, OSL pits, information obtained during the restoration works and earlier explorative pits (Lee Schofield, RSPB, personal communication 7/08/2019).

Electromagnetic radar waves are reflected on subsurface discontinuities characterised by variations in dielectric permittivity, electrical conductivity and magnetic permeability. These material properties allow conclusions on water and ion content, porosity, grain size assemblage, and grain packing and orientation (Neal, 2004; Cassidy, 2008). Thus, the radargrams and core data allowed identification of several facies types and surfaces at a range of scales corresponding to sedimentary and morphological units which were mapped in GIS. The spatial distribution of these facies, their absolute elevation and their depth relative to the current floodplain surface were used to reconstruct planform styles and stages of floodplain evolution. Projected gradient of channels and surfaces, their aspect as well as their geometry and dimensions were employed to infer flow directions and continuity. The latter was challenging due to the spacing between GPR lines relative to the dimensions of the identified units and the gaps in the survey associated with the current channel.

3.2 Optically stimulated luminescence (OSL) dating and dose rate determination

A total of six samples for optically stimulated luminescence (OSL) dating were collected in March 2023 from fine-grained (silt and sand) alluvial units and sandy interbeds within coarser-grained units exposed in two pits excavated into the floodplain and a NW-facing cutbank at the toe of an alluvial fan (Fig. 3). The locations were chosen after analysis of the GPR data to provide age constraint for radar facies II and III as well as lateral fan activity. Sampling was carried out at several depths in pits 1 and 2 in alignment with the encountered stratigraphy whereby sampling of the coarsest units was limited by the aperture size of the tubes. Following the approach of Pope et al. (2008), sections were cleaned back with a trowel prior to light-tight stainless-steel tubes (3 cm in diameter and 20 cm in length) being gently tapped horizontally into targeted fine-grained units. Once filled with sediment, the tube was capped on the outer side to prevent accidental light exposure before being carefully extracted, followed by plugging also its inner end with a plastic cap and sealing with duct tape. Each tube was then given a unique identification code and placed in airtight sample bags to preserve field moisture content. Following the extraction of each tube, a background sample (~300 g) of sediment representative of a 50 cm three-dimensional sphere was collected directly around the sampling point for dose rate determination. Finally, key sample details including longitude, latitude, altitude and burial depth from the top of the section and unique identification code were recorded.

All luminescence samples were processed at the Nordic Laboratory for Luminescence dating (Risø, Denmark), following the methodology outlined by Murray et al., (2021). Environmental dose rate measurements were performed using high resolution gamma spectrometry (Murray et al., 1987; 2018), on sub-samples cast into a fixed geometry. Radionuclide concentrations can be found summarised in Table S1. OSL measurements were performed in a Risø OSL Reader (Bøtter-Jensen et al., 2010), on coarse grains, using a standard SAR protocol for quartz (Murray and Wintle, 2000; 2003) as illustrated by Table S2, and a post-IR IRSL SAR protocol (Thiel et al., 2011) for k-feldspar as shown in Table S3. The De estimates and ages obtained from the k-feldspar are presented in Table S4, while those for quartz can be found in section 3.2 (Table 1). The full details of the analysis are outlined in the supplementary information file.

3.3 Planimetric channel change

A sequence of Uncrewed Aerial Vehicle (UAV) flights were undertaken before restoration, in 2015, and after restoration in 2016, 2017, 2018, 2020 and 2023 to acquire sets of oblique, overlapping Red Green Blue (RGB) images at low flow. A variety of DJI UAV platforms were used, including a Phantom 2 Vision (Williams et al., 2017), Phantom 4, Phantom 4 RTK and an L1 sensor mounted on a Matrice 300 (MacDonell et al., 2023). For each survey, a set of targets were distributed across the site and observed using Real Time Kinematic Global Navigation Satellite System (RTK-GNSS) survey. The images were processed using structure-from-motion photogrammetry (Smith et al., 2015), using Pix4D software. For each survey, the three-dimensional root mean square error at check point targets was <0.1 m. The extent of the wet channel was digitised from the orthomosaic that was produced from each survey.

4. Results and interpretation

4.1 GPR facies

Analysis of the radargrams revealed several facies across the study area, many of which could be identified in core logs. These were then classified into 10 classes based on their spatial relation and dimensions (Fig. 4). While some cores terminated in wet fills of former channels, none reached the groundwater table and thus all surfaces are interpreted as dominantly changes in stratigraphy.

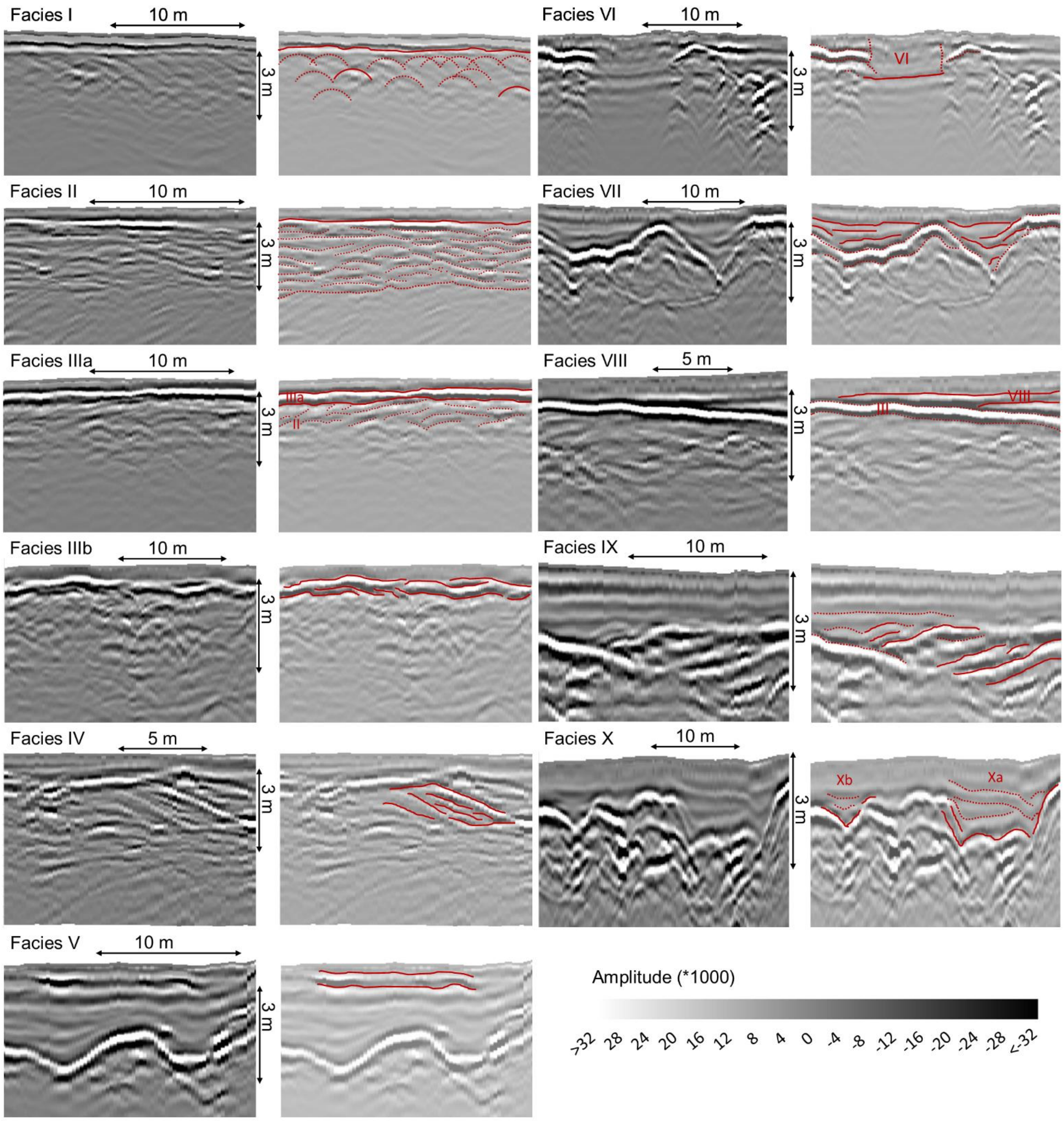

Figure 4. Radar facies identified at The Swindale Beck floodplain. Solid lines are associated with the facies in question while dotted lines show neighbouring or internal reflections.

4.1.1 Facies I – Till

This radar facies is laterally continuous with an undulating upper surface (Fig. 4). The latter can be indistinct but is often indicated by diffraction hyperbolae near the upper boundary which may represent glacial cobbles and boulders. This facies can contain point reflectors at greater depth but is otherwise relatively unstructured and signal attenuation is high. It can be found at depth across the entire floodplain, although in the upstream area F its upper boundary can be up to only one metre below the surface (Fig. 5).

Słowik (2011) suggests such zones of dense diffraction hyberbolae align with changes in lithology within glacial deposits while others have associated them with glacial boulders and cobbles within till (Bridge et al., 1995; Pedersen and Clemmensen, 2005) where the clay matrix can result in high signal attenuation (Ékes and Hickin, 2001). Thus, radar facies I has been interpreted as till of the Dimlington or Loch Lomond Stadials, consisting of silty clay with gravel to boulders (Millward, 2003). While this facies has not been cored, it has been encountered at depth during the restoration works (George Heritage, personal communication 26/06/2019).

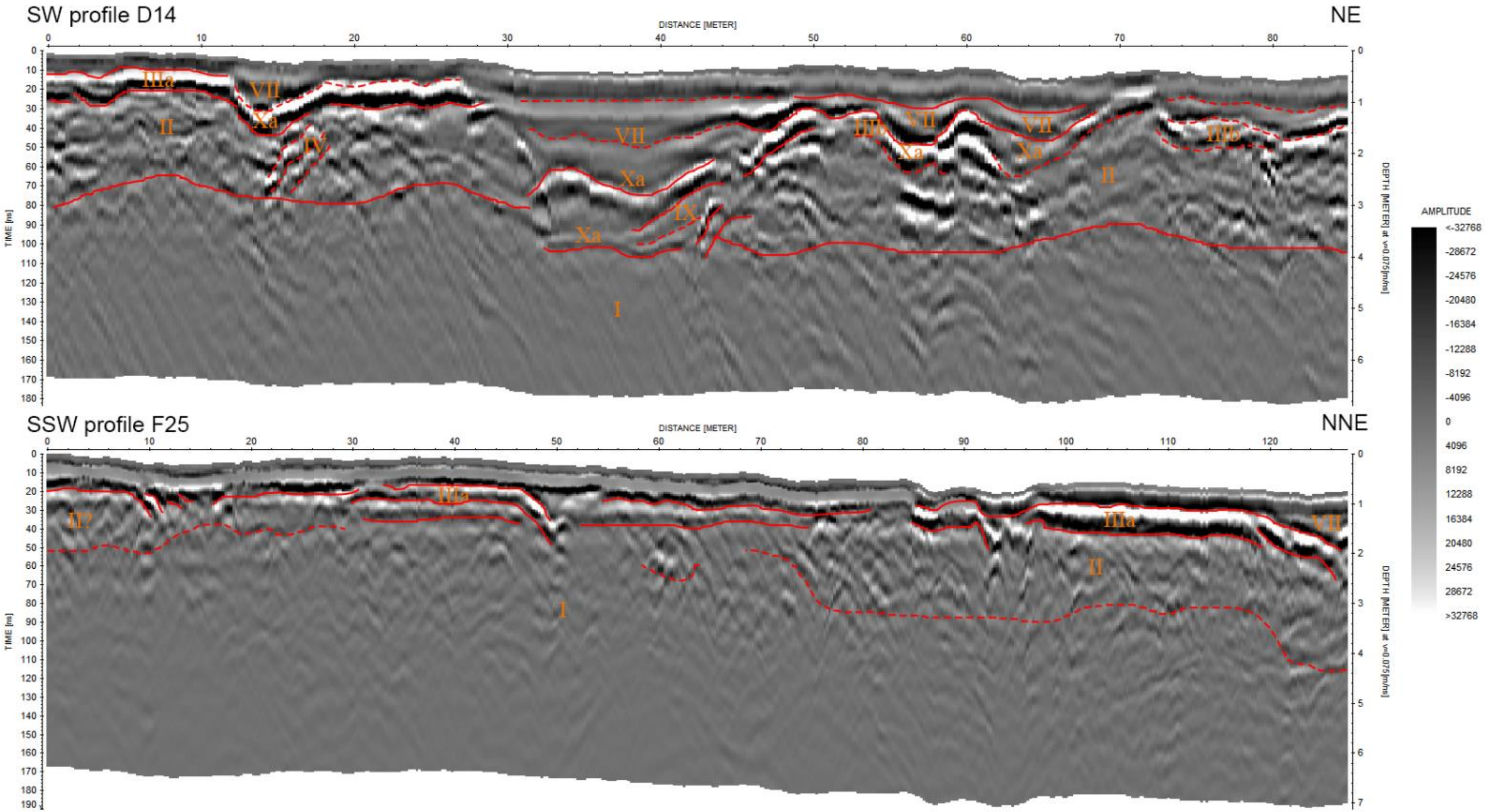

Figure 5. Radargrams of profiles D14 (top) and F25 (bottom) with radar facies annotated in Roman by numerals. Broken lines indicate less clear boundaries between facies or internal structures within a radar facies.

4.1.2 Facies II – Braidplain

This is a laterally continuous radar facies consisting of subparallel reflectors with a wavy appearance and some crossbedding (Fig. 4). In places it includes discontinuous concave reflectors and sub parallel dipping reflections. The facies' upper boundary is undulating and concordant, and appears to be notably lower (e.g. in places more than 1m) below the present floodplain surface in area C compared to the rest of the site (Fig. 6). Its vertical extent typically varies between 2 to 3.5 m with a distinct increase in upvalley direction in area E (Fig. 7). Apart from the western part of the upvalley area F, it is present throughout the study site (Figs. 5 and 8a).

Radar facies II has been interpreted as an aggrading braidplain with medium-sized channels, lateral accretion and channel fills over several storeys. In area D channels are larger (e.g., > 5 m) which might indicate a transition to a wandering planform. Based on depth correlation this facies has been just reached in cores such as 1 or 7 which suggest composition of sandy subrounded gravel (Fig. 9). Very similar radar facies collected by other studies on floodplains have been confirmed as being associated with braidplains (Vandenberghe and van Overmeeren, 1999; Baines et al., 2002; Słowik, 2012a).

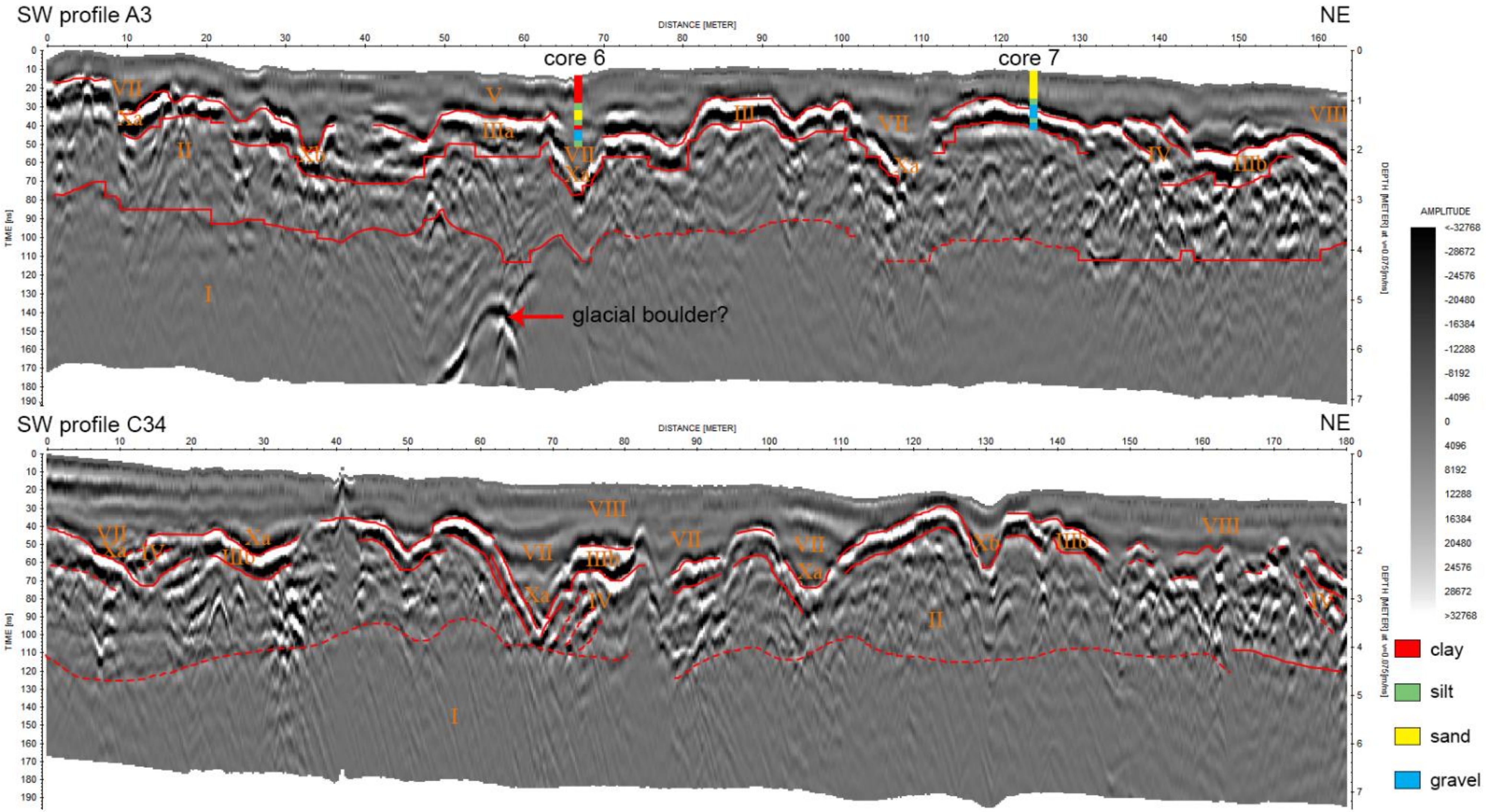

Figure 6. Radargrams of profiles A3 (top) and C34 (bottom) with radar facies annotated in Roman by numerals. Broken lines indicate less clear boundaries between facies or internal structures within a radar facies. Where applicable the location of cores is shown with simplified indication of grainsize. For more details on the cores, see Figure 9.

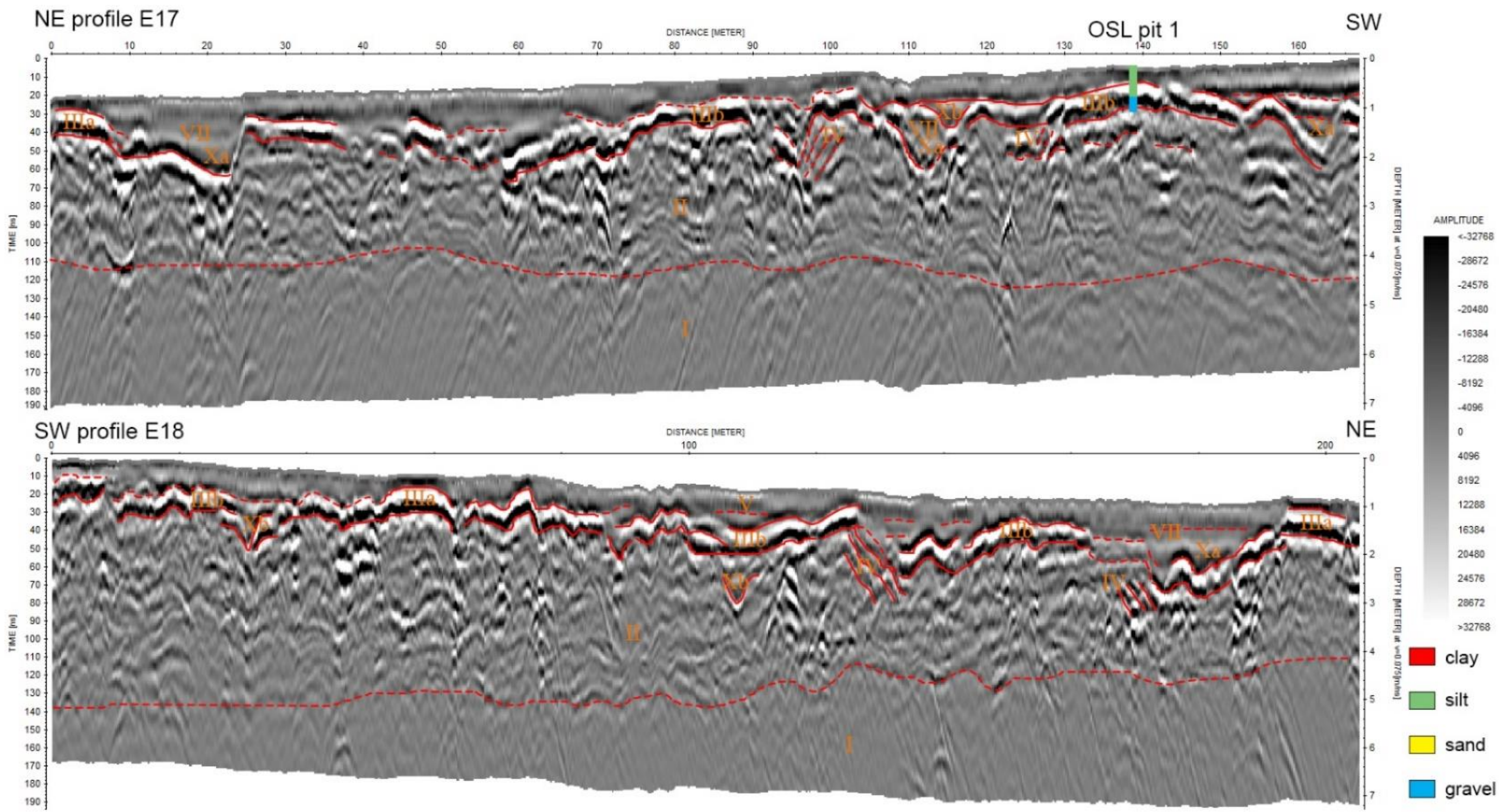

Figure 7. Radargrams of profiles E17 (top) and E18 (bottom) with radar facies annotated in Roman by numerals. Broken lines indicate less clear boundaries between facies or internal structures within a radar facies. Where applicable the location of OSL pits is shown with simplified indication of grainsize. For more details on the stratigraphy, see Figure 11.

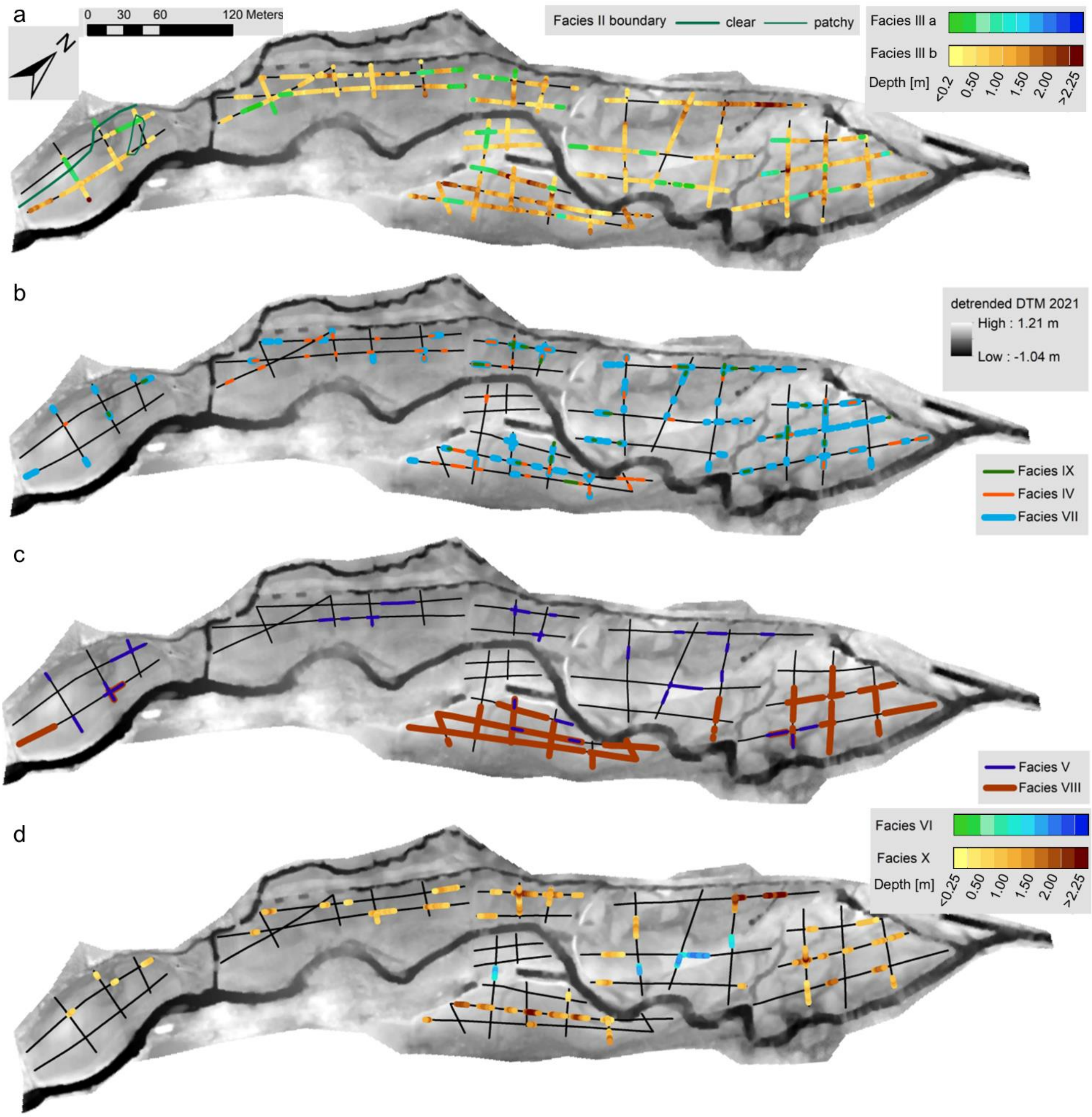

Figure 8. Spatial distribution of radar facies across study site in Swindale. a) Depth of upper boundary of facies III and southwestern limit of the underlying facies II. Location of facies VII, IV and IX, and facies VIII and V are shown in b) and c) respectively. d) Depth of upper boundary of facies associated with channels (X and VI). Where facies are stacked only depths for the uppermost facies are given. Background DTM detrended for valley slope is based on data from the National Lidar Programme 2021 (Open Government Licence).

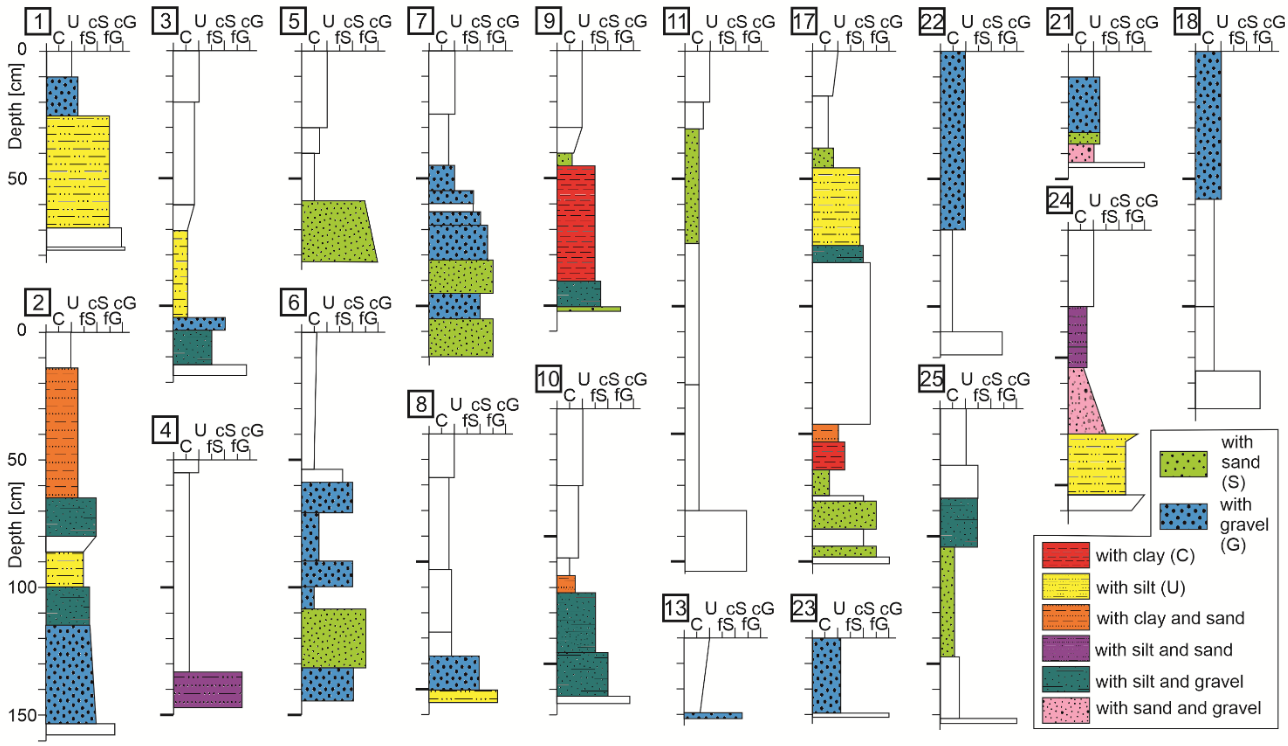

Figure 9 Stratigraphic profiles of 19 soil cores taken along radar profiles at Swindale in August 2019 (for the precise location see Fig. 3). All cores are displayed with the same depth scale. Grainsize is shown on the horizontal axis as C – clay, U – silt, fS – fine sand, cS – coarse sand, fG – fine gravel and cG – coarse gravel. Where the dominant grain size is mixed with substantial amounts of other grain sizes this is indicated by patterns (see legend).

4.1.3 Facies III – Wandering planform deposits

This facies is characterised by a laterally moderately continuous (from several metres to tens of metres), strong reflector which forms the mostly concordant upper boundary (Fig. 4). It can be subdivided into two sub-facies, a) radar facies IIIa which is largely planar or lightly undulating and b) the more undulating radar facies IIIb. Facies IIIa is 0.5 - 1.25 m thick and is laterally terminated by downlap or onlap on other type III facies. Vertical stacking of this facies happens occasionally, e.g. at profile E18 (Fig. 7). Facies IIIb typically has a thickness of less than one metre and is laterally consistent with other type III facies while the lower boundary commonly baselaps onto radar facies II. Both sub-groups of radar facies III are widespread across the entire study site with their deepest occurrence in area C as well as in association with deep palaeochannels in area D and C (Figs. 5, 6 and 8a).

These facies have been reached by numerous cores which indicate a mixture of gravel of various calibre with sand and small cobbles for facies IIIa (cores 1, 5, Fig. 9) while facies IIIb is dominated by coarse sand and fine to medium, subrounded gravel, in places well sorted and layered (cores 3, 7, 9, 10). Comparable radar signals have been interpreted as bedload sheets (IIIa) or low-angle downstream accretion deposits (IIIb) in wandering rivers (Wooldridge and Hickin, 2005). Bridge et al. (1995) found similar facies to our facies IIIb and associated them with lateral accretion of point bars. These facies resemble the morphology and grain size characteristics of contemporary wandering single-or multithreaded rivers (e.g. Wooldridge and Hickin, 2005; Schwendel et al., 2010). Hereby radar facies IIIa represents flat-topped gravel berms with down valley propagation of individual units while radar facies IIIb represents associated small-sized chute channels and bar deposits.

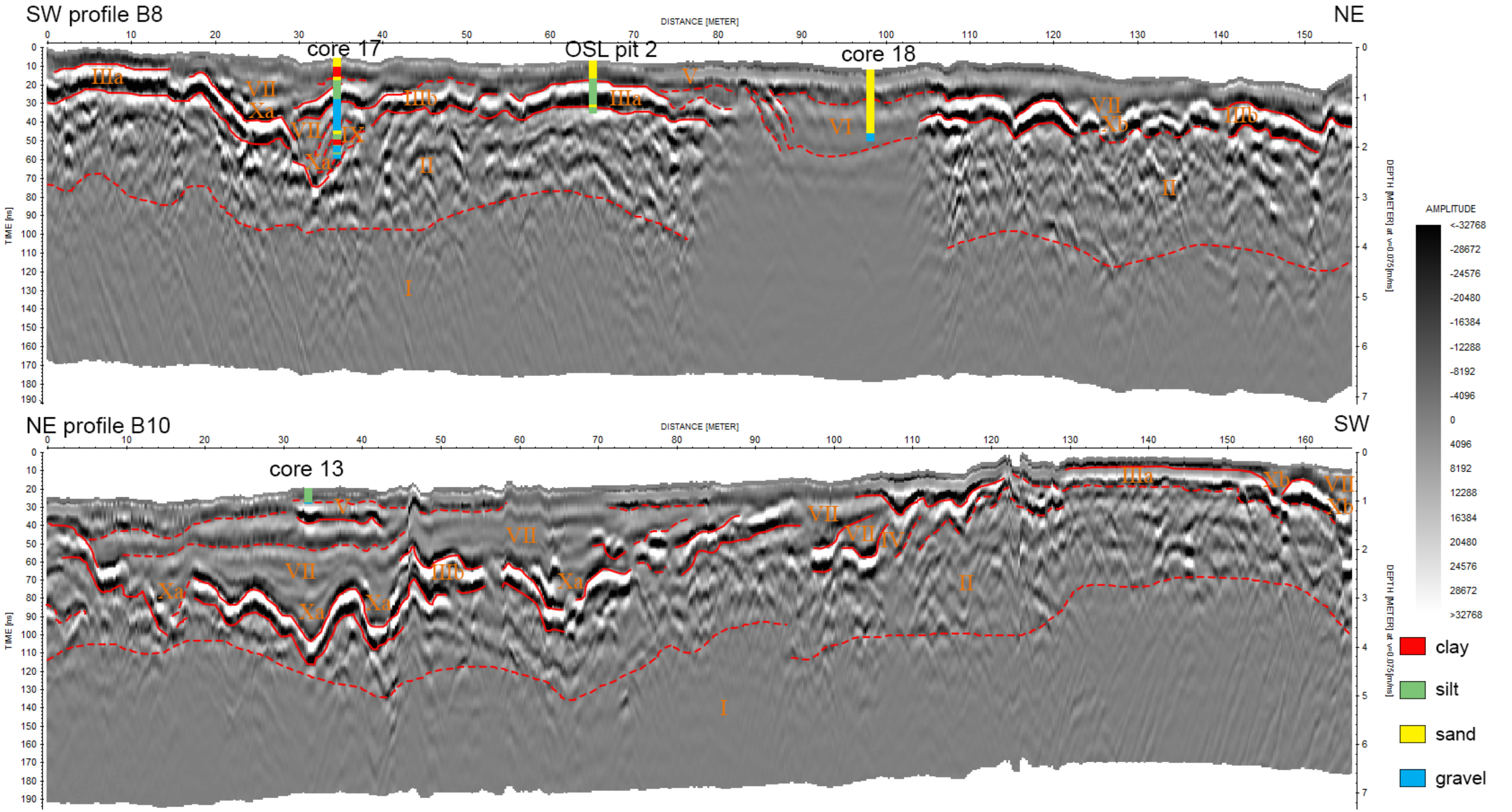

Figure 10. Radargrams of profiles B8 (top) and B10 (bottom) with radar facies annotated in Roman by numerals. Broken lines indicate less clear boundaries between facies or internal structures within a radar facies. Where applicable the location of cores and OSL pits is shown with simplified indication of grainsize. For more details on the stratigraphy, see Figures 9 and 11.

4.1.4 Facies IV – Bar margin lateral accretion deposits

This radar facies consists of multiple oblique parallel reflectors which dip at low angles (10°-20°), often towards concave reflectors in radar facies II (Fig. 4). It has been interpreted as a series of lateral accretion sediments on bar edges, e.g. a point bar in profile E17 (Fig. 7), associated with medium-sized channels particularly common in areas C, D and E (Figs. 5, 6 and 8b).

Such radar facies have been found to form accretion surfaces of compound bars in braided systems (Lunt et al., 2004; Hickin et al., 2009; Słowik, 2012a) while Bridge et al. (1995) identified similar dipping low-amplitude reflectors as lower point bar gravels and sands of a single-thread meander bend.

4.1.5 Facies V – coarse splay/ compaction

Radar facies V is characterised by a planar, horizontal low-amplitude, near-surface reflector with a concordant upper boundary (Fig. 4). The lower boundary is concordant or onlapping onto a variety of other facies. Lateral extent is limited although this facies may be in places disguised by the ground wave. It can be considered of small vertical extent (<0.5 m) and contains well rounded particles up to coarse gravel calibre as evident in cores 13 and 18 (Fig. 9). Facies V can be found in all areas of the study site (Fig. 8c).

Based on the core data, two interpretations are possible. This facies can be interpreted as coarse, superficial flood splay deposits forming a coherent layer of gravel, perhaps thickening in topographic depressions as in profile B10 and core 13 (Figs. 9 and 10). On the other hand, profile B7 and core 18 show a much less coherent distribution of medium gravel clasts but the surface has been artificially compacted during artificial infilling of redundant channels (see facies VI below). Słowik (2014a) identified horizontal and wavy reflectors as being associated with a “toughened cartroad” surface and associated construction works (Słowik, 2012a). While this documented radar signal bears some similarity to radar facies V, the coarse grain size of this layer makes it more distinguishable from the facies below which is not the case at Swindale.

4.1.6 Facies VI – artificial channel fill

This facies, apart from some ringing noise, is largely reflection free. Its upper boundary is concordant, often with radar facies V, while the planar lower boundary is identified by a high-amplitude, concordant, planar reflector (Figs. 4 and 10) although signal attenuation can be high. The facies has a distinct lateral boundary with various other facies suggesting an erosional contact. This facies is restricted to locations in areas B and C where the straight channel, infilled in during the restorations works, was situated (Fig. 8d).

Given this information interpretation as artificial channel fill comprising fine material intermixed with organic matter, gravel and individual cobbles is straightforward. The lack of internal structure and strong attenuation is typical for highly conductive material (Ékes and Hickin, 2001). Cores 18 and 22 (Fig. 9) indicate a tendency of fining with depth until the coarse, armoured former channel bed is reached at depths of 1.1 m and 1.25 m respectively.

4.1.7 Facies VII – Channel fill

Radar facies VII consists of planar to lightly undulating or dipping, weak parallel reflectors with an onlapping lower boundary (Fig. 4). The facies is laterally constrained by high-amplitude, concave reflectors (typically facies X, e.g Figs. 5, 6 and 10). It can be found across the entire study site but is most common in the down-valley areas A, B and C (Fig. 8b). It has been reached by numerous cores which indicate that alternate layering of mostly moderately sorted coarse (e.g., fine gravel, coarse sand) and dark fine sediments (e.g., silt, fine sand) whereby the coarser fractions are mostly angular and the finer layers may contain substantial organic matter or show signs of hydromorphy such as mottling and nodules (cores 2, 6, 10, 17 in Fig. 9). Core 8 revealed some weak laminations within the depth range of this radar facies.

This facies has been interpreted as fill of topographic depressions such as inactive channels with fine backwater deposits and episodically coarser bedload from floods but may also include some bar sediments near the channel edges. The presence of organic matter is typical in such a setting (Bristow et al., 1999), likely contributing to anoxic conditions in stagnant waters. This interpretation coincides with that of other studies of very similar facies, e.g. Słowik (2012a) and Dara et al. (2019) interpreted them as channel fill sediments although in the latter they were lacking the distinct internal structure found here.

4.1.8 Facies VIII – Backwater deposits

This facies is characterised by laterally extensive planar horizontal parallel reflectors of low amplitude (Fig. 4). Its upper boundary is often not clear in the radargrams but cores indicate a clear boundary to mostly coarser sediments above at 0.15-0.25 m depth (e.g., cores 3, 4, 7, 11, Fig. 9). At the respective depth these cores show grainsizes from silty clay to silt. The lower boundary of radar facies VIII onlaps onto other facies (e.g., type III) or is concordant with radar facies VII (Fig. 6). Thickness of this facies is greatest in area C where it is also most widespread while its vertical extent is less and more variable in the other areas (Fig. 8c).

The fine nature and horizontal stratigraphy suggest a low energy depositional environment without episodical coarse flood deposits such as backwaters or a temporary lake. The coarsening and thinning of this facies away from area C and the southern part of area A suggests approach of the margins of such a backwater basin. Similar radar facies but with higher proportion of organic material were interpreted by Słowik (2013) and Słowik (2014b) as organic fill of a stagnant water basins on the Obra River and as homogeneous fine palaeochannel fill by Elznicová et al. (2023).

4.1.9 Facies IX – Prograding channel deposits

Radar facies IX consists of gently inclined oblique sigmoidal reflectors downlapping and onlapping onto other radar facies, e.g. facies X and facies III respectively (Fig. 4). Spatially it is often associated with facies VII and X (Figs. 8 and 10). The facies has been reached by cores 2, 11, 17 and possibly 24, which all agree on grain sizes in the gravel range (Fig. 9). Core 17 suggests some layered strata but dipping angle could not be measured.

Based on the radargrams this facies has been interpreted as prograding channel deposits possibly associated with lateral or downstream accretion or bar slipface deposition in the larger channels. Similar radar facies have been interpreted as pointbar migration (Vandenberghe and van Overmeeren, 1999; Dara et al., 2019), downstream bar accretion deposits (Wooldridge and Hickin, 2005; Elznicová et al., 2023) or prograding splay deposits (Bristow et al., 1999).

4.1.10 Facies X – Erosional surfaces

Radar facies X is characterised by laterally discontinuous, concave high-amplitude reflectors (Fig. 4). Symmetric, asymmetric, more semi-circular or trapezoidal as well as compound forms have all been grouped into this facies, but it has been sub-divided into two sub-facies based on lateral extent: sub-facies Xa with more than 5 m and sub-facies Xb for smaller features. This radar facies is laterally mostly associated with facies II and III.

Sub-facies Xa is present in all areas but particularly frequent along profiles C34 (Fig. 6), B10 (Fig. 10), E17 and E18 (Fig. 7) while sub-facies Xb is equally distributed across the site apart from area B (Fig. 8d). Areas B, C and D harbour the deepest examples of the facies while they are rather shallow below the contemporary floodplain surface in area F (Fig. 5). Core data indicates that it consists of gravel deposits (cores 3, 10 and 11 in Fig. 9). Geometry and grain size lead to the interpretation of this facies as erosional surfaces such as channel bottom and coarse bar deposits which corresponds with interpretation of similar radar facies by others (Ékes and Hickin, 2001 (facies 8); Heinz and Aigner, 2003; Hickin et al., 2009; Słowik, 2012a; Dara et al., 2019 (facies 5)).

4.1.11 Vertical floodplain accretion

Apart from the cores situated in artificial channel fill, all cores show vertical accretion sediments from the surface to a depth ranging from 0.05 m to 0.3 m (Fig. 9).

4.2 Luminescence dating

The measured OSL ages for the sample from the toe of the alluvial fan AF1 shows the oldest age with 5.22±0.35 ka (Table 1). It comes from the fourth lowest distinctive layer within this profile (Fig. 11) and so may not represent the newest date of fan activity at this point, however, the calibre of coarse clasts in the layers above prevented sampling for OSL. The ages of samples representing radar facies III (OSL1.2 and OSL2.3: ~1.7 ka) and the transition between facies II and III (OSL1.1 and OSL2.2: ~3.65 ka) correspond well between the two pits. However, given the discrepancy between feldspar and quartz ages as expressed in high IR_{50}/OSL ratios (Table 1) this is likely coincidental.

Table 1: Quartz equivalent doses, total dose to quartz and luminescence ages for the Swindale samples ((n_a) number of aliquots accepted; (n_r) number of aliquots rejected; w.c. -water content)

Lab./ sample code	**Location**	**Depth (cm)**	**w.c. (%)**	**Quartz OSL**			**Total dose rate**	**Final age**	**Signal resetting**	
							Quartz	OSL	Ratio	Sufficiently well bleached
				D_e (Gy)	(n_r)	(n_a)	Gy/ka	(ka)	IR_{50}/OSL	
231401 OSL 1.1	Pit 1	81	26	9.69 ± 0.62	1	26	2.68 ± 0.11	3.61 ± 0.29	3.66	
231402 OSL 1.2	Pit 1	50	18	5.03 ± 0.68	0	13	2.93 ± 0.13	1.72 ± 0.25	7.18	
231403 OSL 2.1	Pit 2	98	26	2.72 ± 0.49	2	17	2.98 ± 0.14	0.99 ± 0.19	1.11	✓
231404 OSL 2.2	Pit 2	76	19	11.3 ± 0.9	2	15	3.08 ± 0.15	3.68 ± 0.36	1.45	
231405 OSL 2.3	Pit 2	54	18	5.44 ± 0.86	1	20	3.19 ± 0.15	1.71 ± 0.28	n.a.	

231406 OSL 4.1	Pit 4	41	23	16.1 ± 0.8	0	26	3.08 ± 0.14	5.22 ± 0.35	1.08	✓

It has been well documented that partial bleaching of the luminescence signal prior to deposition can lead to significant age overestimation in some fluvial settings (Jain et al., 2004; Wallinga, 2008; Murray et al., 2012; Weckwerth et al., 2013; Colarossi et al., 2015; Chamberlain and Wallinga, 2018). This problem results from the very rapid attenuation of light spectra through the water column, leaving insufficient energy to fully reset the luminescence signal (Berger, 1990); the addition of suspended sediment further enhances the effect (Berger and Luternauer, 1987). The potential for bleaching of sand sized grains in fluvial settings is known to be further reduced by short transport distances as opportunities for light exposure are limited (Cunningham et al., 2014). Bleaching would appear to be enhanced by longer transport distances, possibly due to the potential for numerous subaerial exposures during ephemeral storage episodes on the surface of river bars (Stokes et al., 2001). However, this does not appear to be universal guarantee of sufficient signal resetting, as mixing with older or poorly reset material remobilised from localised terrace erosion during high discharge storm events is also more likely to have taken place over longer transport distances (Rittenour, 2008; McGuire and Rhodes, 2015).

With no absolute assurance of sufficient signal resetting in fluvial environments it is vitally important to not take luminescence ages obtained from fluvial sediments at face value. Of the variety of methods routinely used to assess the bleaching status of such samples we have opted to employ the unambiguous bleaching properties of the quartz and potassium feldspar signals to test the validity of the ages presented in this study.

It has been observed that the post-IR signals in feldspar bleach much more slowly and are therefore much more difficult to reset than the IR_{50} signal, and that the IR_{50} resets much more slowly than the OSL signal in quartz (Poolton et al., 2002; Jain and Ankjærgaard, 2011; Murray et al., 2012). It is therefore possible to draw conclusions regarding the completeness of signal resetting at the time of deposition in the quartz by comparing it to the harder to bleach feldspar. This is an approach that has been successfully demonstrated by Möller and Murray (2015), Alexanderson et al. (2024) and Thompson et al. (2024). The post-IR feldspar ages significantly overestimate the corresponding quartz OSL ages in all samples with the exception of OSL 2.3 (Table 1). Unfortunately, this sample yielded no usable feldspar, and it is not possible to make any further comment on the signal resetting in this case. A comparison of the IR_{50}/OSL ages for samples OSL 1.1 and OSL 1.2 (Pit 1) also shows a significant overestimation, and therefore we cannot comment conclusively on the degree of signal resetting in these samples. The two samples are however stratigraphically consistent with each other. In Pit 2 there appears to be a stratigraphic inversion in the quartz ages. Comparing the IR_{50}/OSL ages for the samples that yielded K-rich feldspar, we see that in OSL 2.1 this ratio is 1.11; as this is within 2σ of unity we can conclude that the OSL signal in this sample was sufficiently well reset prior to burial. For sample OSL 2.2 the IR_{50}/OSL age ratio is 1.45, indicating that the quartz signal might not be as well bleached in this instance, and we should trust the age of the deepest sample OSL 2.1 more (Table 1, Fig. 11). In the case of sample OSL 4.1 the ratio is much closer to unity (1.08), and we can be confident that the OSL signal was fully reset.

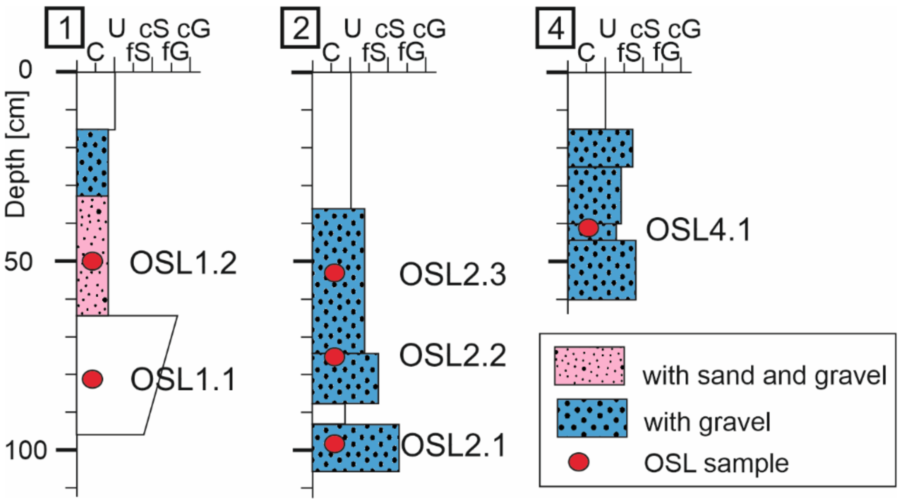

Figure 11. Stratigraphic profiles of the three pits (1, 2 and 4) dug to extract OSL samples at Swindale in March 2023 (for the precise location see Fig. 3). All profiles are displayed with the same depth scale. Grainsize is shown on the horizontal axis as C – clay, U – silt, fS – fine sand, cS – coarse sand, fG – fine gravel and cG – coarse gravel. Where the dominant grain size is mixed with substantial amounts of other grain sizes this is indicated by patterns (see legend).

5. Floodplain development

Based on the combination of core, radar data and chronometric data several stages of floodplain development can be reconstructed (Fig. 12). In the localised context of upper Swindale such development is conditioned by the outcrop of an andesitic sill downstream of the study site (Fig. 2) which provides local base level control. This limits erosion within at least parts of the study site and has preserved stratigraphic evidence of floodplain evolution. Furthermore, moraines and alluvial fans in the valley are sources for sediment supply to the studied reach (Fig. 1c).

Radar facies I forms the base of the floodplain across the entire study site and is very likely associated with till. The depth of its upper boundary increases down-valley to up to 5 metres below the current floodplain surface. The age of this till is not known precisely, although McDougall (2013) suggests that during the Loch Lomond Stadial (12.9-11.7 cal. ka BP) glaciers extended as far as the study site as evidenced by moraines preserved to the east of area A (Fig. 1c).

5.1 Stage 1

After the Loch Lomond Stadial (12.9 -11.7 cal. ka BP), the initial stage of floodplain development coincided with the partial incision and concomitant burial of glacial till (facies I) by an evolving braided fluvial system. This system occupied almost the entire study site (apart from the northern part of area F) (Fig, 8a) and is characterised by channel and bar sequences (facies II and IV). The chronology of sandy gravels that constitute the basal and stratigraphically lower units of facies II has yet to be fully resolved. Nevertheless, a single OSL age estimate (c. 5.22 $\pm$ 0.35 ka) from an alluvial fan (AF1) suggests that deposition of the basal and lower sandy gravel occurred before the middle Holocene. Assuming this is the case, the oldest sandy gravel units are potentially analogous to radiocarbon dated terraced gravels in Bowderdale, in the Howgill Fells which were emplaced before 6763-7005 cal. BP (6070 $\pm$ 70 BP: SRR-318) (Miller, 1991) and the Upper Langden, in the Bowland Fells where deposition occurred prior to 5316-5573 cal. BP (4680 $\pm$ 80 BP: WIS-1614) (Miller, 1991).

The delivery of coarse-grained sediment to the valley floor via steep tributary valleys culminated in the progradation of alluvial fans across the margins of the braidplain (profile F25, 63-71 m, Fig. 5) during the mid-Holocene (c. 5.22 $\pm$ 0.35 ka). This phase of fan progradation appears to have initiated the local development of a wandering planform in the lower area E and area D of the braidplain evidenced by deep (buried) larger, possibly more permanent channels with point bars and associated accretion structures (facies IV, Fig. 8b). It is not known if the floodplain environment was characterised by sustained aggradation or spatially selective reworking during the post-middle Holocene to late Holocene period. Following the middle Holocene, aggradation varied significantly in regional catchments. At Colley Moor, Northumbria, a radiocarbon date from a silty sand unit inset within soliflucted till suggests that in Coe Burn, a phase of fine-grained alluvium took place after 4259-4584 cal. BP (3920±70 BP:BETA-28982) (Macklin et al., 1991). By comparison, there is no compelling evidence of mid-Holocene aggradation in catchments in the Howgill Fells, Bowland Fells, and the Southern Uplands (Chiverrell et al., 2007 and references therein). The scale of human activity and land use-change within the study area during the late Holocene is not known. Nevertheless, palaeolimnological evidence indicates that woodland clearances across the Lakeland Fells were minor and localised until c. 5200 cal. BP (Pennington, 1991), whereas the late Bronze Age to early Iron age (2700-2800 cal. BP) and particularly the late Iron Age and Romano-British periods (2300-1500 cal. BP) witnessed a significant increase in the distribution and intensity of clearances (Pennington, 1978; Hodgkinson et al., 2000; Chiverrell et al., 2004). It is possible that the combination of localised clearances and the shift to wetter conditions around 5.2 ka, 4.2 ka, 3.6 ka, and 2.8 ka (Charman, 2010; Roland et al., 2015) led to intermittent aggradation in the braidplain environment in the period between the post-middle Holocene and start of the late Holocene.

A single OSL age (0.99 $\pm$ 0.19 ka) from the lower sandy gravel unit of Facies II and the presence of several storeys of braidchannels suggest that a significant aggradation occurred across the floodplain started approximately 1000 years BP. Assuming this is the case, the lower sandy gravel unit is potentially analogous to lower terraced gravels that were the emplacement in the lower Ribble catchment c.1000 cal. BP (Chiti, 2004) and in Kirtle Water, Southern Uplands between 1000 and 750 cal. BP (Tipping, 1995). The scale of human activity and land use-change occurring within the study area during this period is not known. Nevertheless, palaeolimnological evidence and pollen data indicate that significant woodland clearances occurred across the Lake District (Pennington, 1991; 1997; Dumayne-Peaty and Barber, 1998), the Howgill Fells (Cundill, 1976), and Rotten Bottom in the Southern Uplands (Tipping, 1999) in response to a growing rural economy that coincide with the Norse settlement period (1200-950 cal. BP) (Winchester, 1987). With woodland clearance from upland areas around Swindale, the steep tributary systems are likely to have transferred coarse- and fine-grained sediment to the floodplain zone (cf. Harvey, 2002). Nevertheless, the sustained rates of floodplain aggradation almost certainly reflect the progressive reworking and remobilization of glacial, paraglacial, and fluvial sediment stored upstream coupled with the downstream base level control exerted by the andesitic sill downstream of the study site and sediment storage opportunities linked to valley-floor configuration at Swindale (cf. Passmore and Macklin, 2000; Chiverrell et al., 2007).

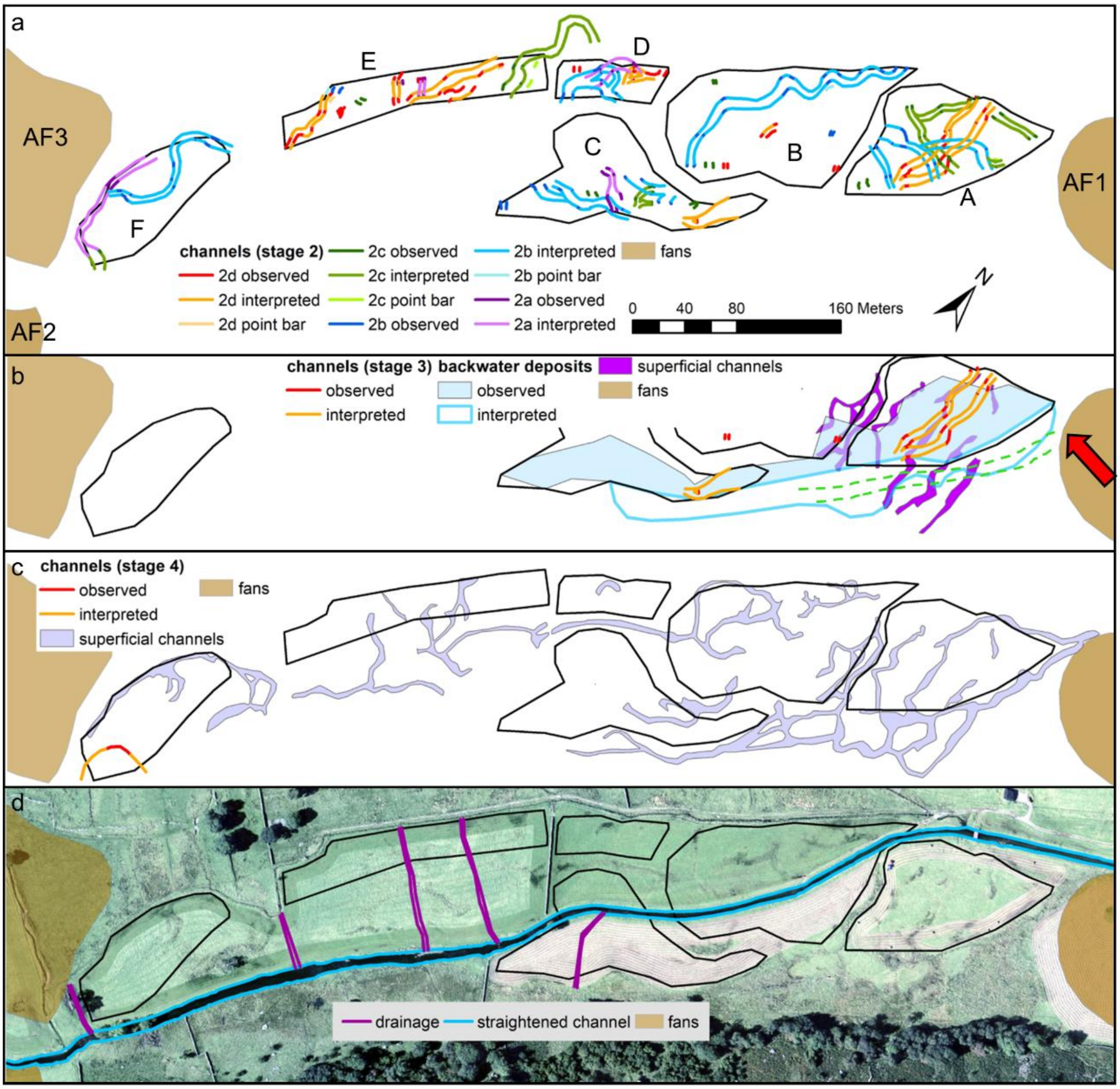

Figure 12. Stages of sequential floodplain and channel development at Swindale based on radar analysis. A) Stage 2, a multi-thread or wandering planform with several channel system stacked. Identified substages indicate depth below the contemporary floodplain with substage 2a being the lowest. These substages are not necessarily correlated between the different areas (labelled A-F). Alluvial fans (AF) are potential sources of sediment. B) Stage 3 characterised by northerly drainage across areas A and B, likely caused by blockage of a

channel on the south-eastern valley side (indicated by green dotted lines) for example by activity of an alluvial fan 1 (red arrow). Backwater deposits have been found in areas A, B and C but have likely extended further South-east. C) Stage 4, a single thread or low-order multi-thread planform with its main channel largely outside the surveyed areas. Erosion along the toe of AF1 has enabled a shift to a south-easterly drainage route in the lower study area. Many superficial channels on the associated floodplain are still detectable from aerial imagery, constituting tributary channels and remnants from earlier stages. D) Stage 5, an artificially straightened channel with floodplain drainage. High resolution (25 cm) vertical aerial imagery from 2009 has been sourced from Getmapping using EDINA Aerial Digimap Service.

5.2 Stage 2

The second stage of floodplain evolution is characterised by a low-order multi-thread or single-thread wandering planform (Fig. 12a). It is mainly associated with radar facies III, representing bedload sheets, bars and transient chute channels, as well as lateral accretion deposits (IV). In addition, channels of various size are preserved (X) together with prograding coarse bar migration sediments (IX) and fine channel fills (VII). A geochronology for this stage of floodplain development is lacking. Nevertheless, an OSL age of 0.99 ± 0.19 ka generated for facies II places the formation of facies III and hence the second stage of floodplain development within a late Holocene timeframe.

The shift from stage 1 to stage 2 is distinct in the GPR data and in places associated with considerable coarsening of the sediment calibre, e.g. facilitated by deposition of coarse bedload sheets over finer bar top sediments (Figs. 5, 6, 7 and 10). However, whether these bars have been created in a braiding or wandering environment is often not resolved and thus the transition between the two stages might have been much more gradual. Such a shift could be attributed to changes in sediment supply due to climatic alterations as well as anthropogenic land use change, albeit with some lag time (Chiverrell, 2006; Larsen et al., 2013). However, given the limited dating control, it is not known if changes in sediment supply occurred during the 9th century AD (c.1000 cal. BP) or the following centuries AD. The erosion of soils and sediment in several Lakeland catchments is evidenced by the increased delivery of fine-grained sediment to several Lake systems c. 1000 cal. BP and 500 cal. BP (Chiverrell, 2006 and references therein; Shen et al., 2008; Hatfield and Maher, 2009). In other areas of the Lake District, significant gullying and erosion linked to the exploitation of hillslopes culminated in alluvial fan progradation in Blind Tarn Moss (Easedale) and Derwent catchment, Borrowdale after 895-725 cal. BP (860±40 BP: SUERC-6686) (Chiverrell et al., 2007) and 621- 515 cal. BP (534±45 BP: OXA-7751) (Wild et al., 2001), respectively. By comparison, in the central Southern Uplands, erosion resulting from the exploitation of hillslopes led to fan aggradation in Dalveen Pass (Lowther Hills) and Nitties Burn after 485-520 cal. BP (466±25 BP: SUERC-4704) and 310-460 cal. BP (330±70 BP: BETA-95478) (Chiverrell et al., 2007), respectively. The temporal variability in sedimentation between catchments is likely to reflect differing levels of landscape (in-)stability within catchments (Chiverrell et al., 2008) coupled with variable preservation potential of stream deposits and alluvial fan gravels in valley floor environments (e.g. Lewin et al., 2005). Within Swindale, the continued availability of (glacial, paraglacial, and fluvial) sediment in upstream storage zones coupled and localised reworking of floodplain and alluvial fan sediments offers a potential explanation for aggradation spanning the 9th and 15th centuries AD (1000-500 BP). Additionally, the valley configuration created a ‘buffer’ effect leading to significantly greater reach-scale storage and preservation of floodplain sediments (e.g. Lewin et al., 2005).

Multiple levels of channels of varying dimensions have been found across the entire study site which allows distinction of several storeys. These substages indicated in Figure 12a refer to the depth below the contemporary floodplain surface of identified channel systems within each area. Elevation and channel dimensions were used to attempt the matching of substages between neighbouring areas. However, spatial gaps in the survey prevent correlating these systems across the entire study site but they nevertheless indicate floodplain architectures and possible channel planforms. Changes in channel dimensions may be attributed to variation in sediment supply, e.g. the incision of a deep channel along the toe of the fan AF3 (stage 2a in Fig. 12a), and thus the ratio between transport capacity and sediment supply of the system (Harvey, 2002). Large channels at depth (Fig. 8d) have been recognised on both sides of the valley (areas D, C and B) implying a dynamic system that used the full width of the valley. Erosion in more recent stages and anthropogenic interventions such as the excavation of the straight channel and, more recently, the re-meandered channel have removed evidence of floodplain development in the central parts of the valley. However, it is remarkable that no traces of deep or large channels have been found along the valley axis, e.g. in the western part of area C (profiles C29-32) and the eastern part of area B (profiles B7-9, B11 and B12; e.g. Fig. 10). The detrended DEM (Fig. 8) indicates a topographic high along this axis in areas B and C and radar facies III is consistently deepest below surface level along the edges of the valley (profiles C36, C34, B10 and D14 respectively; Figs. 5, 6 and 10), hereby indicating a gradient away from the valley centre axis. While the contemporary topographic high in the valley centre may be associated with levees and overbank deposition along the former straight channel (Reid, 2015; Wightman and Schofield, 2021), an explanation for such an arrangement at depth is less straightforward. Potentially differential till deposition at the margin of the Younger Dryas glaciation might have favoured drainage along the valley edges where lateral fans allowed. As a result, the main channels may have shifted at intervals between a train of channels on either the NW or SE edges of the valley downstream of the narrow point created by the alluvial fans AF2 and AF3 at the up-valley end of the study site (Fig. 1c). Only in area A, likely beyond the margin of Younger Dryas glaciation (Fig. 1c), there is clear evidence of cross-valley drainage as well as potentially one substantial channel in area B (stage 2d in Fig. 12a). The reconstruction of drainage in area A suggests roughly E and NE drainage direction for most of this stage with a distinct shift to a northward drainage for the uppermost channels. This might be the result of blockage of a main channel at the eastern valley edge, for example by activation of alluvial fan AF1 there. Such an episode could have led to rerouting of drainage and temporary impoundment there, which is supported by apparent fading and fragmentation of radar facies III at the down valley end of profiles C34 (Fig. 6), C35 and C36 and leads to development stage 3 in the downstream part of the study site.

5.3 Stage 3

The third stage is characterised by backwater deposits (radar facies VIII) extending across much of areas C and A and several N-S aligned channels across area A some of which are still evident in the contemporary floodplain surface (Fig. 12b). Such a shift to a northerly direction of the drainage in the lower study area may be explained by bio-geomorphic alterations (e.g. beaver dams) or the mentioned westward extension of the alluvial fan AF1 and the resulting blockage of the previous southeastern alluvial drainage route. While the age of deposition at the toe of AF1 (pit 4) is much older than the developments in stage 3, other parts of the fan may have been active at different times. The ensuing impoundment would have rerouted channels to the North and created the substantial downvalley thickening deposits associated with radar facies VIII. It is possible that gradual fill of the basin has led to avulsion further upstream and reoccupation/ scour of a large channel through area B (stage 2b in

Fig. 12a). Whether this episode was triggered by a general reactivation of fan AF1, bio-geomorphic agents or avulsions and drainage changes within is unclear.

Channel fills (radar facies VII) as part of channel migration and abandonment within a wandering river floodplain are present as well during this stage, however, this facies varies from the backwater facies VIII in its smaller horizontal extent, lateral onlap on channel facies X and presence of alternating layers. In contrast, facies VIII is less structured, fine throughout (at least in area A) and often situated over channel fills (Fig. 6).

5.4 Stage 4

After incision of a new south-eastern channel along the toe of AF1, it is likely that the main channel reversed to the SE valley side again (Fig. 12c). The previous N-S aligned spill channels across area A of stage 3 were filled (radar facies VII) or drained the floodplain. More recently after the channel restoration works some of these channels have been reactivated, albeit with a reversed flow direction towards the newly excavated channel, which they meet at an obtuse angle (Fig. 8).

The radargrams show only the margins of the stage 4 main channel system (e.g., profiles B9, A5, C33, E19 and F27) suggesting a spatially constraint, likely single-thread or low-order multithread channel system and associated floodplain development. The reconstructed large bend on the SW end of area F (radar facies X on profile F24, Fig. 8d) shows erosional contact with adjacent facies and may be associated with this system. During this stage vertical accretion sediments have been deposited across the study site suggesting a reduction in coarse sediment supply and channel stabilisation. Some superficial coarse splay deposits laid down during floods are found across the entire site (radar facies V, Fig. 8c).

Figure 12c also shows an array of superficial channels evident only from radargrams as well as those also visible from aerial photography. These are likely to have linked tributaries to the main channel prior to floodplain drainage.

5.5 Stage 5

The last stage that is evident from the GPR survey is the anthropogenic realignment of Swindale Beck (Fig. 12d) and the insertion of drainage pipes in the floodplain. The fill of the straightened channel during the restoration works 2016 can be clearly seen as radar facies VI (Fig. 8d). Some sediments associated with radar facies V (Fig. 8c) may present compacted soil as a result of the use of heavy machinery.

5.6 Stage 6

Figure 13 shows the planform dynamics of the extent of the active channel, defined as the mosaic of the low flow wet channel and unvegetated bars, since the 2016 channel realignment. Bank erosion at the outer banks of meander bends has resulted in channel migration, with the highest rates along the more sinuous set of meanders along Phase 1 (downstream segment of the scheme). The 2023 survey shows one area of bifurcation, upstream of the point where the realigned channel crosses the pre-restoration channel. Here, the realigned channel bifurcated during a high-flow event and a knickpoint worked upstream from the pre-restoration channel, which had not been infilled along this reach of former channel. However, during low flows this new channel remains dry. Overall channel adjustment has been gradual and during the seven-year post-realignment monitoring period.

Figure 13. Planform change at Swindale Beck following restoration. Channel extent for each year is based on low-flow, wet channel extent from orthoimages produced using UAV acquired images that were processed using SfM photogrammetry. The polygons showing the extent of the active channel are each partly transparent; where they overlay a mix of colours from different years is shown.

6. Implications for river management

The analysis of floodplain stratigraphy using GPR has been shown to allow reconstruction of key stages of the evolution of river styles and floodplain formation at Swindale. River management, including the planning and design of river restoration projects can draw various benefits from such an approach. In this context, GPR provides a spatially extensive, time and cost-efficient appraisal of floodplain stratigraphy using a non-invasive approach (Szuch et al., 2006) suitable for sensitive habitats, like the 'Site of Special Scientific Interest' at Swindale. Knowledge of stratigraphy provides opportunities to facilitate sustainable river management approaches in several ways. Firstly, it allows the identification of past river styles and their interpretation in relation to sediment sources and lateral constraints (e.g., alluvial fans). Słowik (2015) showed how geophysical floodplain investigation along with analysis of historical maps and aerial imagery can lead to the design of sustainable restoration schemes. Knowing the sensitivity of a fluvial system to local influences and the ensuing effects on planform change in the past are important to be considered for designing a restored system that will fulfil the restoration objectives in a changing climate. Not all restoration schemes aim to emulate a past river style and channel configuration but are driven by specific objectives. At Swindale, the restoration design aimed to primarily increase biodiversity in the valley while preserving the protected hay meadows and associated grassland plant communities (Wightman and Schofield, 2021) and thus opted for a single-thread channel form with increased channel sinuosity, creation of point bars and pool-riffle morphology. A secondary objective was not to increase sediment flux downstream, due to drinking water abstraction from the Beck in the reach immediately downstream of the realignment scheme (Wightman and Schofield, 2021). The development of a secondary high-flow channel in 2022 (Fig. 13) shows that under current climate and sediment supply conditions a wandering planform could develop and that implementation of such a system during the restoration design process may have been feasible, had the objectives been different. This study has demonstrated that at Swindale over the last 1000 years there was a trajectory of river styles from braiding over a wandering planform to single-thread with episodes of impoundment which can be linked with historic changes in climate and sediment supply. Hence, this fluvial system appears to be relatively responsive to extrinsic changes. This is an important consideration when creating channel configurations that are sustainable and functional in predicted climate change conditions. While the gaps in our survey, largely imposed by recent engineering works, prevented the reconstruction of a coherent channel network for the individual stages of development, GPR surveys can be used to create three-dimensional subsurface models (e.g. Heinz and Aigner, 2003; Kostic and Aigner, 2007) which may serve as a basis for hydraulic modelling of flow and sediment conveyance for comparison with planned restoration options. Whilst our results demonstrate clear evidence for a former multi-thread channel system at the study site, we do not claim that this is necessarily suitable for the current river system. However, knowledge of past river styles gained from GPR data may help to select an appropriate channel morphology that is aligned with the contemporary and future flood and sediment supply regime and may go beyond the often aesthetically favoured meandering design (Podolak and Kondolf, 2016). Additionally, in wider river management context, the appreciation of the sedimentary consequences of past anthropogenic actions (e.g., channel straightening in stage 5) for the floodplain may support adaptive planning for prospective works (e.g., water diversions) (Lewin, 2013).

Secondly, for river restoration programs knowing the precise position, depth and thickness of gravel/ cobble bodies in the floodplain allows dimensioning and positioning of restored channels (Schneider et al., 2011). The presented GPR data distinguished between grain size fractions of sediment and precisely outlined former channels which could be linked in many instances. This investigation also shows that many of the palaeochannels were not evident from aerial photography or lidar commonly used for their detection, or masked by engineering works of stage 5. At Swindale the routing of the new channel of the restoration scheme was in the lower part of the study site (around areas A, B and C) guided by the presence of channels on the floodplain interpreted from lidar and aerial photography while in the upper part (areas D, E and F) a more sinusoidal course was favoured. The post-restoration channel development (stage 6, Fig. 13) shows for the latter a lower level of channel dynamics and Wightman and Schofield (2021) noted a paucity of gravels in the restored channel. A GPR survey across the site before the restoration works would have enabled identification of the location of single-thread or low order multi-thread channels of stage 4, their connectivity at depth and dimensions and thus may have avoided the need to artificially construct gravel bars.

Thirdly, spatially coherent information on floodplain stratigraphy reveals location and quantity of sustainable and local sources of coarse substrate potentially needed during restoration works (e.g., sediment replenishment), which are as cut-and fill structures often not evident from surface topography (Huber et al., 2019). GPR surveys can also indicate suitable conditions for wetlands (Szuch et al., 2006), characterise gravel aquifers (Doetsch et al., 2010; 2012). Furthermore, they allow avoidance of undesired sedimentary bodies (e.g., mining deposits, landfill) and the, often neglected, assessment of vertical hyporheic connectivity (Sparacino et al., 2019; Howard et al., 2024).

Floodplain roughness and vegetation have been shown to impose some limits on efficient surveying and thick and clay rich top layers may attenuate the radar signal and reduce penetration depth (Annan, 2008). Nevertheless, our results clearly demonstrate that in suitable conditions and particularly for larger areas, GPR surveys can provide a more spatially coherent, non-invasive imaging of the floodplain compared to coring and can be a valuable tool to guide the river restoration practitioner towards recreating an appropriate channel morphology.

7. Conclusions

This study demonstrates the utility of GPR surveys to identify floodplain evolution and spatio-temporal river planform development at Swindale Beck under the influence of various conditioning factors such as bedrock geology, glacial deposits, activity of alluvial fans and anthropogenic activity. This led to the reconstruction of five main stages of floodplain development over the entire study site with an additional stage for the south-eastern part where alluvial fan activity appears to have triggered a more complex drainage pattern. OSL dating placed the transition from a braiding river style to a dominantly wandering planform within the last 990 years. The response of river planform to the conditioning influences in such a timeframe is relevant for river restoration schemes which aim to create sustainable conditions in a changing climate. Thus, we argue that understanding of past river styles, which can be efficiently obtained from GPR surveys, provides practitioners with important information for deciding design options. For the example of Swindale it is demonstrated how subsurface imaging also allows appraisal of hyporheic connectivity, location of gravel resources and identification of depth and geometry of a wider range of palaeochannels than can be obtained from surface data. While a full absolute chronology for each stage of development was not permitted with the design of OSL sampling and thus beyond the scope of this paper, it would be desirable for linking past environmental conditions with the corresponding geomorphological processes at each stage. Furthermore, closer spacing of GPR survey profiles and data acquisition prior to fragmentation of the floodplain by restoration works may allow for better reconstruction of palaeotopography. This may in turn serve as a basis for hydrodynamic modelling in order to test the suitability of past river styles under contemporary sedimentary and hydrological conditions.

8. Acknowledgements

We are grateful to Lee Schofield (RSPB Haweswater) for providing information on the restoration scheme and allowing site access. We would also like to thank George Heritage for introduction to the site. ACS received financial support for field data collection from York St John University. RDW received funding for fieldwork from a British Society for Geomorphology Early Career Grant and a Royal Academy of Engineering Industrial Secondment (RAE ISS1617/46). We thank staff and students from Aberystwyth University and the University of Glasgow who have contributed to topographic surveys to monitor the realignment scheme, especially Lucy Daniels, Craig MacDonell and Kenny Roberts.

9. References

Alexanderson, H., Möller, P., Jain, M., Knudsen, M.F., Larsen, N.K., Perić, Z.M., Søndergaard, A.S., Thompson, W., 2024. Coupled luminescence and cosmogenic nuclide dating of postglacial deflation surfaces and sand drift on a raised ice-contact delta at Veinge, SW Sweden. Quaternary Geochronology, 80, p.101500.

Annan, A.P., 2008. Electromagnetic principles of ground penetrating radar. In: H.M. Jol (Ed.), Ground Penetrating Radar Theory and Applications. Elsevier Science & Technology, Amsterdam, pp. 3-40.

Antonarakis, A.S., Milan, D.J., 2020. Uncertainty in parameterizing floodplain forest friction for natural flood management, using remote sensing. Remote Sensing, 12(11), p.1799.

Arnaud, F., Piégay, H., Béal, D., Collery, P., Vaudor, L., Rollet, A.J., 2017. Monitoring gravel augmentation in a large regulated river and implications for process-based restoration. Earth Surface Processes and Landforms, 42(13), pp.2147-2166.

Baines, D., Smith, D.G., Froese, D.G., Bauman, P., Nimeck, G., 2002. Electrical resistivity ground imaging (ERGI): a new tool for mapping the lithology and geometry of channel-belts and valley-fills. Sedimentology 49(3), 441-449.

Beechie, T. J., Sear, D.A., Olden, J.D., Pess, G.R., Buffington, J.M., Moir, H., Roni, P., Pollock, M.M., 2010. Process-based Principles for Restoring River Ecosystems. BioScience, 60(3), 209-222.

Beniston, M., 2009. Trends in joint quantiles of temperature and precipitation in Europe since 1901 and projected for 2100. Geophysical Research Letters, 36(7).

Berger, G.W., 1990. Effectiveness of natural zeroing of the thermoluminescence in sediments. Journal of Geophysical Research: Solid Earth, 95(B8), 12375-12397.

Berger, G.W., Luternauer, J.J., 1987. Preliminary field work for thermoluminescence dating studies at the Fraser River delta, British Columbia. Geological Survey of Canada Paper, 87, 901-904.

BGS, 2013. Geology Map 10k. Tiles: ny40ne, ny41se, ny50nw, ny51sw. British Geological Survey.

Bickerdike, H.L., Evans, D.J.A., Ó Cofaigh, C., Stokes, C.R., 2016. The glacial geomorphology of the Loch Lomond Stadial in Britain: a map and geographic information system resource of published evidence. Journal of Maps 12(5), 1178-1186.

Biron, P. M., Buffin-Bélanger, T., Larocque, M., Choné, G., Cloutier, C.-A., Ouellet, M.-A., Demers, S., Olsen, T., Desjarlais, C., Eyquem, J., 2014. Freedom Space for Rivers: A Sustainable Management Approach to Enhance River Resilience, Environmental Management, 54(5), 1056-1073.

Bøtter-Jensen, L., Thomsen, K.J., Jain, M., 2010. Review of optically stimulated luminescence (OSL) instrumental developments for retrospective dosimetry. Radiation Measurements, 45, 253–257.

Bravard, J.P., Petts, G.E., 1996. Human impacts on fluvial hydrosystems. In The Fluvial Hydrosystems (pp. 242-262). Dordrecht: Springer Netherlands.

Bridge, J.S., Alexander, J.A.N., Collier, R.E.L., Gawthorpe, R.L., Jarvis, J., 1995. Ground-penetrating radar and coring used to study the large-scale structure of point-bar deposits in three dimensions. Sedimentology 42(6), 839-852.

Bristow, Skelly, Ethridge, 1999. Crevasse splays from the rapidly aggrading, sand-bed, braided Niobrara River, Nebraska: effect of base-level rise. Sedimentology 46(6), 1029-1047.

Brousse, G., Liébault, F., Arnaud-Fassetta, G., Breilh, B., Tacon, S., 2021. Gravel replenishment and active-channel widening for braided-river restoration: The case of the Upper Drac River (France). Science of the Total Environment, 766, p.142517.

Brown, A.G., Keough, M., 1992. Holocene floodplain metamorphosis in the Midlands, United Kingdom. Geomorphology, 4(6), pp.433-445.

Brown, T., 1997. Clearances and clearings: deforestation in Mesolithic/Neolithic Britain. Oxford Journal of Archaeology, 16(2), pp.133-146.

Cassidy, N.J., 2008. Ground penetrating radar data processing, modelling and analysis. In: H.M. Jol (Ed.), Ground Penetrating Radar Theory and Applications. Elsevier Science & Technology, Amsterdam, pp. 141-172.

Chamberlain, E., Wallinga, J., 2018. Fluvial sediment pathways enlightened by OSL bleaching of river sediments and deltaic deposits. Earth Surface Dynamics Discussion, 1-29.

Charman, D.J., 2010. Centennial climate variability in the British Isles during the mid–late Holocene. Quaternary Science Reviews, 29 (13-14), 1539–1554.

Chiti, B., 2004. Holocene fluvial and marine influences and sediment interactions in the lower Ribble valley, Lancashire, UK. Unpublished PhD thesis, University of Stirling.

Chiverrell, R.C., Coombes, P.M.V., Blundell, A.C., Thompson, G., Bailey, W., 2004. Peatlands of the south Lake District. In: Chiverrell, R.C., Plater, A.J., Thomas, G.S.P. (Eds.), The Quaternary of the Isle of Man and Northwest England: Field Guide. Quaternary Research Association, London, pp. 155–175.

Chiverrell, R., 2006. Past and future perspectives upon landscape instability in Cumbria, northwest England. Regional Environmental Change, 6, 101-114.

Chiverrell, R.C., Harvey, A.M., Foster, G.C., 2007. Hillslope gullying in the Solway Firth- Morecambe Bay region, Britain: responses to human impact and/or climatic deterioration? Geomorphology, 84, 317–343.

Chiverrell, R.C., Harvey, A.M., Hunter, S.Y., Millington, J. Richardson, N.J., 2008. Late Holocene environmental change in the Howgill Fells, Northwest England, Geomorphology, 100, (1–2), 41-69.

Church, M., Ferguson, R.I., 2015. Morphodynamics: Rivers beyond steady state. Water Resources Research, 51(4), 1883-1897.

Colarossi, D., Duller, G.A.T., Roberts, H.M., Tooth, S., Lyons, R., 2015. Comparison of paired quartz OSL and feldspar post-IR IRSL dose distributions in poorly bleached fluvial sediments from South Africa. Quaternary Geochronology, 30, 233-238.

Cundill, P.R., 1976. Late Flandrian vegetation and soils in Carlingill valley, Howgill Fells. Transactions Institute of British Geographers, 4, 301–309.

Cunningham, A.C., Wallinga, J., Hobo, N., Versendaal, A.J., Makaske, B., Middelkoop, H., 2014. Does deposition depth control the OSL bleaching of fluvial sediment? Earth Surface Dynamics Discussions, 2(2), 575-603.

Curran, J.C., Cannatelli, K.M., 2014. The impact of beaver dams on the morphology of a river in the eastern United States with implications for river restoration. Earth Surface Processes and Landforms, 39(9), pp.1236-1244.

Dadson, S.J., Hall, J.W., Murgatroyd, A., Acreman, M., Bates, P., Beven, K., Heathwaite, L., Holden, J., Holman, I.P., Lane, S.N., O'Connell, E., Penning-Rowsell, E., Reynard, N., Sear, D., Thorne, C., Wilby, R., 2017. A restatement of the natural science evidence concerning catchment-based 'natural' flood management in the UK. Proceedings of the Royal Society A: Mathematical, Physical and Engineering Sciences, 473(2199), 20160706.

Dara, R., Kettridge, N., Rivett, M., Krause, S., Gomez-Ortiz, D., 2019. Identification of floodplain and riverbed sediment heterogeneity in a meandering UK lowland stream by ground penetrating radar. Journal of Applied Geophysics, 103863.

Doetsch, J., Linde, N., Coscia, I., Greenhalgh, S.A., Green, A.G., 2010. Zonation for 3D aquifer characterization based on joint inversions of multimethod crosshole geophysical data. Geophysics, 75(6), G53-G64.

Doetsch, J., Linde, N., Pessognelli, M., Green, A.G., Günther, T., 2012. Constraining 3-D electrical resistance tomography with GPR reflection data for improved aquifer characterization. Journal of Applied Geophysics, 78, 68-76.

Dumayne-Peaty, L., Barber, K.E., 1998. Late Holocene vegetation history, human impact and representativity variations in northern Cumbria, UK. Journal of Quaternary Science, 13, 147–164.

Ékes, C., Hickin, E.J., 2001. Ground penetrating radar facies of the paraglacial Cheekye Fan, southwestern British Columbia, Canada. Sedimentary Geology, 143(3), 199-217.

Elznicová, J., Kiss, T., von Suchodoletz, H., Bartyik, T., Sipos, G., Lenďáková, Z., Fačevicová, K., Pavlů, I., Kovárník, J., Matys Grygar, T., 2023. Was the termination of the Jizera River meandering during the Late Holocene caused by anthropogenic or climatic forcing? Earth Surface Processes and Landforms 48(4), 669-686.

Entwistle, N., Heritage, G. and Milan, D., 2018. Flood energy dissipation in anabranching channels. River Research and Applications, 34(7), pp.709-720.

Garcia de Leaniz, C., 2008. Weir removal in salmonid streams: implications, challenges and practicalities. Hydrobiologia, 609(1), pp.83-96.

Gourry, J.-C., Vermeersch, F., Garcin, M., Giot, D., 2003. Contribution of geophysics to the study of alluvial deposits: a case study in the Val d'Avaray area of the River Loire, France. Journal of Applied Geophysics, 54(1–2), 35-49.

Gowan, C., Fausch, K.D., 1996. Long-term demographic responses of trout populations to habitat manipulation in six Colorado streams, Ecol. Appl., 6, 931–946.

Grabowski, R.C., Gurnell, A.M., Burgess-Gamble, L., England, J., Holland, D., Klaar, M.J., Morrissey, I., Uttley, C., Wharton, G., 2019. The current state of the use of large wood in river restoration and management. Water and Environment Journal, 33(3), pp.366-377.

Groisman, P.Y., Knight, R.W., Easterling, D.R., Karl, T.R., Hegerl, G.C., Razuvaev, V.N., 2005. Trends in Intense Precipitation in the Climate Record. Journal of Climate, 18(9), 1326-1350.

Gumiero, B., Mant, J., Hein, T., Elso, J., Boz B., 2013. Linking the restoration of rivers and riparian zones/wetlands in Europe: Sharing knowledge through case studies, Ecol. Eng., 56, 36–50.

Hankin, B., Metcalfe, P., Beven, K., Chappell, N. A., 2019. Integration of hillslope hydrology and 2D hydraulic modelling for natural flood management. Hydrology Research, 50(6), 1535-1548.

Hannaford, J., Buys, G., 2012. Trends in seasonal river flow regimes in the UK. Journal of Hydrology, 475, 158-174.

Harper, D.M., Ebrahimnezhad, M., Taylor, E., Dickinson, S., Decamp, O., Verniers, G., Balbi, T., 1999. A catchment-scale approach to the physical restoration of lowland UK rivers. Aquatic Conservation: Marine and Freshwater Ecosystems, 9(1), pp.141-157.

Harvey, A.M., 2002. Effective timescales of coupling within fluvial systems. Geomorphology, 44(3), 175-201.

Hatfield, R.G., Maher, B.A., 2009. Holocene sediment dynamics in an upland temperate lake catchment: climatic and land-use impacts in the English Lake District. The Holocene, 19(3), 427-438.

Heinz, J., Aigner, T., 2003. Three-dimensional GPR analysis of various Quaternary gravel-bed braided river deposits (southwestern Germany). Geological Society, London, Special Publications, 211(1), 99-110.

Heritage, G., Large, A., Milan, D., 2021. A field guide to British Rivers. John Wiley & Sons.

Hester, E.T. and Gooseff, M.N., 2011. Hyporheic restoration in streams and rivers. Stream restoration in dynamic fluvial systems: Scientific approaches, analyses, and tools, 194, pp.167-187.

Hickin, A.S., Kerr, B., Barchyn, T.E., Paulen, R.C., 2009. Using Ground-Penetrating Radar and Capacitively Coupled Resistivity to Investigate 3-D Fluvial Architecture and Grain-Size Distribution of a Gravel Floodplain in Northeast British Columbia, Canada. Journal of Sedimentary Research, 79(6), 457-477.

Hodgkinson, D., Huckerby, E., Middleton, R., Wells, C.E., 2000. The Lowland Wetlands of Cumbria, North West Wetlands Survey 6. Oxford Archaeology North, Oxford, pp. 360-362.

Holden, J., Evans, M.G., Burt, T.P., Horton, M., 2006. Impact of land drainage on peatland hydrology. Journal of Environmental Quality, 35(5), pp.1764-1778.

Howard, B.C., Baker, I., Blackmore, M., Kettridge, N., Ullah, S., Krause, S., (2024). Restoring the Liver of the River. In: Krause, S., Hannah, D., Grimm, N. (Eds.), Ecohydrological Interfaces, Wiley, Chichester, pp. 355-390.

Hubbs, C.L., Greeley, J.R., Tarzwell, C.M., 1932. Methods for the improvement of Michigan trout streams, Bull. Inst. Fish. Res. 1, Univ. of Mich. Press, Ann Arbor.

Huber, E., Anders, B., Huggenberger, P., 2019. Imaging scours in straightened and braided gravel-bed rivers with ground-penetrating radar. Near Surface Geophysics, 17(3), 263-276.

Jain, M., Murray, A.S., Botter-Jensen, L., 2004. Optically stimulated luminescence dating: how significant is incomplete light exposure in fluvial environments? [Datation par luminescence stimulée optiquement: quelle signification en cas de blanchiment incomplet des sédiments fluviatiles?]. Quaternaire, 15(1), 143-157.

Jain, M., Ankjærgaard, C., 2011. Towards a non-fading signal in feldspar: insight into charge transport and tunnelling from time-resolved optically stimulated luminescence. Radiation Measurements, 46(3), 292-309.

Johnson, E.A.G., 1954. Land drainage in England and Wales. Proceedings of the Institution of Civil Engineers, 3(6), pp.601-629.

Kondolf, G.M., 2006. River restoration and meanders. Ecology and Society, 11(2).

Kostic, B., Aigner, T., 2007. Sedimentary architecture and 3D ground-penetrating radar analysis of gravelly meandering river deposits (Neckar Valley, SW Germany). Sedimentology, 54(4), 789-808.

Larsen, A., Bork, H.-R., Fuelling, A., Fuchs, M., Larsen, J.R., 2013. The processes and timing of sediment delivery from headwaters to the trunk stream of a Central European mountain gully catchment. Geomorphology, 201(0), 215-226.

Lewin, J., 2010. Medieval environmental impacts and feedbacks: the lowland floodplains of England and Wales. Geoarchaeology, 25(3), pp.267-311.

Lewin, J., 2013. Enlightenment and the GM floodplain. Earth Surface Processes and Landforms, 38(1), 17-29.

Lewin, J., Macklin, M.G., Johnstone, E., 2005. Interpreting alluvial archives: sedimentological factors in the British Holocene fluvial record. Quaternary Science Reviews, 24(16-17), 1873–1889.

Lunn, A.G., 1990. Glacial landforms and sediments in Swindale. Proceedings of the Cumberland Geological Society, 5, 218-220.

Lunt, I.A., Bridge, J.S., Tye, R.S., 2004. A quantitative, three-dimensional depositional model of gravelly braided rivers. Sedimentology, 51(3), 377-414.

MacDonell, C.J., Williams, R.D., Maniatis, G., Roberts, K., Naylor, M., 2023. Consumer-grade UAV solid-state LiDAR accurately quantifies topography in a vegetated fluvial environment. Earth Surface Processes and Landforms, 48(11), 2211-2229.

Macklin, M.G., Passmore, D.G., Stevenson, A.C., Cowley, D.C., Edwards, D.N., O'Brien, C.F, 1991. Holocene alluviation and land-use change on Callaly Moor, Northumberland, England. Journal of Quaternary Science, 6, 225-232.

McDougall, D., 2013. Glaciation style and the geomorphological record: evidence for Younger Dryas glaciers in the eastern Lake District, northwest England. Quaternary Science Reviews, 73, 48-58.

McGuire, C., Rhodes, E.J., 2015. Downstream MET-IRSL single-grain distributions in the Mojave River, southern California: Testing assumptions of a virtual velocity model. Quaternary Geochronology, 30, 239-244.

Medel, I.D., Stubblefield, A.P., Shea, C., 2022. Sedimentation and erosion patterns within anabranching channels in a lowland river restoration project. International Journal of River Basin Management, 20(3), pp.399-409.

Milan, D.J., Petts, G.E., Sambrook, H., 2000. Regional variations in the sediment structure of trout streams in southern England: benchmark data for siltation assessment and restoration. Aquatic Conservation: Marine and Freshwater Ecosystems, 10(6), pp.407-420.

Milan, D.J., Schwendel, A.C., 2021. Climate-change driven increased flood magnitudes and frequency in the British uplands: Geomorphologically informed scientific underpinning for upland flood-risk management. Earth Surface Processes and Landforms, 46(15), 3026-3044.

Miller, J.D., Hess, T., 2017. Urbanisation impacts on storm runoff along a rural-urban gradient. Journal of Hydrology, 552, pp.474-489.

Miller, S.Y., 1991. Soil chronosequences and fluvial landform development. Unpublished PhD thesis, University of Liverpool.

Millward, D., 2003. The Lower Palaeozoic igneous rocks and Quaternary deposits of the area between Haweswater and Shap (part of Sheets 30 and 39, England and Wales), British Geological Survey, Keyworth.

Möller, P., Murray, A.S., 2015. Drumlinised glaciofluvial and glaciolacustrine sediments on the Småland peneplain, South Sweden–new information on the growth and decay history of the Fennoscandian Ice Sheets during MIS 3. Quaternary Science Reviews, 122, 1-29.

Murray, A.S., Helsted, L.M., Autzen, M., Jain, M., Buylaert, J.P., 2018. Measurement of natural radioactivity: Calibration and performance of a high-resolution gamma spectrometry facility. Radiation Measurements, 120, 215–220.

Murray, A.S., Thomsen K.J., Masuda N., Buylaert J.P., Jain M., 2012. Identifying well-bleached quartz using the different bleaching rates of quartz and feldspar luminescence signals. Radiation Measurements, 47, 688-695.

Murray, A., Marten, R., Johnston, A., Martin, P., 1987. Analysis for naturally occurring radionuclides at environmental concentrations by gamma spectrometry. Journal of Radioanalytical and Nuclear. Chemistry, 115, 263–288.

Murray, A., Arnold, L.J., Buylaert, J.P., Guérin, G., Qin, J., Singhvi, A.K., Smedley, R., Thomsen, K.J., 2021. Optically stimulated luminescence dating using quartz. Nature Reviews Methods Primers, 1(1), 1-31.

Murray, A.S., Wintle A.G., 2003. The single aliquot regenerative dose protocol: potential for improvements in reliability. Radiation Measurements 37, 377-381.

Murray, A.S., Wintle, A.G., 2000. Luminescence dating of quartz using an improved single-aliquot regenerative-dose protocol. Radiation. Measurements, 32, 57–73.

Neal, A., 2004. Ground-penetrating radar and its use in sedimentology: principles, problems and progress. Earth-Science Reviews, 66(3), 261-330.

Newson, M.D., Large, A.R., 2006. Natural rivers, hydromorphological quality and river restoration: a challenging new agenda for applied fluvial geomorphology. Earth Surface Processes and Landforms, 31(13), 1606-1624.

Passmore, D.G., Macklin, M.G., 2000. Late Holocene channel and floodplain development in a wandering gravel-bed river: the River South Tyne at Lambley, northern England. Earth Surface Processes and Landforms, 25(11), 1237–1256.

Pedersen, K., Clemmensen, L.B., 2005. Unveiling past aeolian landscapes: A ground-penetrating radar survey of a Holocene coastal dunefield system, Thy, Denmark. Sedimentary Geology, 177(1), 57-86.

Pennington, W., 1978. The impact of man on some English lakes: rates of change. Polskie Archiwum Hydrobiologii, 25, 429–437.

Pennington, W., 1991. Palaeolimnology in the English Lakes—some questions and answers over fifty years. Hydrobiologia, 214, 9–24.

Pennington, W., 1997. History of the vegetation. In Halliday, G. (Ed.). A Flora of Cumbria. Centre for northwest regional studies, University of Lancaster. Bolton: Shanleys, pp. 43-50.

Piégay, H., Darby, S.E., Mosselman, E., Surian, N., 2005. A review of techniques available for delimiting the erodible river corridor: a sustainable approach to managing bank erosion. River Research and Applications, 21(7), 773-789.

Podolak, K., Kondolf, G.M., 2016. The Line of Beauty in River Designs: Hogarth's Aesthetic Theory on Capability Brown's Eighteenth-Century River Design and Twentieth-Century River Restoration Design. Landscape Research, 41(1), 149–167.

Poolton, N.R.J., Ozanyan, K.B., Wallinga, J., Murray, A.S., Bøtter-Jensen, L., 2002. Electrons in feldspar II: a consideration of the influence of conduction band-tail states on luminescence processes. Physics and Chemistry of Minerals, 29, 217-225.

Pope, R., Wilkinson, K., Skourtsos, E., Triantaphyllou, M., Ferrier, G., 2008. Clarifying stages of alluvial fan evolution along the Sfakian piedmont, southern Crete: New evidence from analysis of post-incisive soils and OSL dating. Geomorphology, 94 (1–2), 206-225.

Powers, P.D., Helstab, M., Niezgoda, S.L., 2019. A process-based approach to restoring depositional river valleys to Stage 0, an anastomosing channel network. River Research and Applications, 35(1), pp.3-13.

Prior, J., 2016. Urban river design and aesthetics: a river restoration case study from the UK. Journal of Urban Design, 21(4), pp.512-529.

Ramchunder, S.J., Brown, L.E., Holden, J., 2012. Catchment-scale peatland restoration benefits stream ecosystem biodiversity. Journal of Applied Ecology, 49(1), pp.182-191.

Reid, H.E., 2015. Swindale River Restoration Plan, Environment Agency.

Rittenour, T.M., 2008. Luminescence dating of fluvial deposits: applications to geomorphic, palaeoseismic and archaeological research. Boreas, 37(4), 613-635.

Roland, T.P., Daley, T.J., Caseldine, C.J., Charman, D.J., Turney, C.S.M., Amesbury, M.J., Thompson, G.J., Woodley, E.J., 2015. The 5.2 ka climate event: evidence from stable isotope and multi-proxy palaeoecological peatland records in Ireland. Quaternary Science Reviews, 124, 209–223.

Schneider, P., Vogt, T., Schirmer, M., Doetsch, J., Linde, N., Pasquale, N., Perona, P., Cirpka, O.A., 2011. Towards improved instrumentation for assessing river-groundwater interactions in a restored river corridor. Hydrol. Earth Syst. Sci., 15(8), 2531-2549.

Schwendel, A.C., Fuller, I.C., Death, R.G., 2010. Morphological dynamics of upland headwater streams in the southern North Island of New Zealand. New Zealand Geographer, 66(1), 14-32.

Schwendel, A.C., 2019. Assessment of geomorphological aspects of river restoration strategy at Hull Road Park, York. Report for City of York Council.

Sear, D., Newson, M., Hill, C., Old, J., Branson, J., 2009. A method for applying fluvial geomorphology in support of catchment-scale river restoration planning. Aquatic Conservation: Marine and Freshwater Ecosystems, 19(5), 506-519.

Sear, D.A., 1994. River restoration and geomorphology. Aquatic Conservation: Marine and Freshwater Ecosystems, 4(2), pp.169-177.

Sear, D.A., Newson, M.D., Brookes, A., 1995. Sediment-related river maintenance: the role of fluvial geomorphology. Earth Surface Processes and Landforms, 20(7), 629-647.

Shen, Z., Bloemendal, J., Mauz, B., Chiverrell, R., Dearing, J., Lang, A., Liu, Q., 2008. Holocene Environmental Reconstruction of Sediment-Source Linkages at Crummock Water, English Lake District, Based on Magnetic Measurements. The Holocene, 18, 129-140.

Smith, M.W., Carrivick, J.L., Quincey, D.J., 2015. Structure from motion photogrammetry in physical geography. Progress in Physical Geography, 40(2), 247-275.

Sparacino, M.S., Rathburn, S.L., Covino, T.P., Singha, K., Ronayne, M.J., 2019. Form-based river restoration decreases wetland hyporheic exchange: Lessons learned from the Upper Colorado River. Earth Surface Processes and Landforms, 44(1), 191-203.

Stokes, S., Bray, H.E., Blum, M.D., 2001. Optical resetting in large drainage basins: tests of zeroing assumptions using single-aliquot procedures. Quaternary Science Reviews, 20(5-9), 879-885.

Słowik, M., 2011. Reconstructing migration phases of meandering channels by means of ground-penetrating radar (GPR): the case of the Obra River, Poland. Journal of Soils and Sediments, 11(7), 1262-1278.

Słowik, M., 2012a. Changes of river bed pattern of a lowland river: effect of natural processes or anthropogenic intervention? Geografiska Annaler: Series A, Physical Geography, 94(3), 301-320.

Słowik, M., 2012b. Influence of measurement conditions on depth range and resolution of GPR images: The example of lowland valley alluvial fill (the Obra River, Poland). Journal of Applied Geophysics, 85, 1-14.

Słowik, M., 2013. GPR and aerial imageries to identify the recent historical course of the Obra River and spatial extent of Obrzańskie Lake, altered by hydro-technical works. Environmental Earth Sciences, 70(3), 1277-1295.

Słowik, M., 2014a. Analysis of fluvial, lacustrine and anthropogenic landforms by means of ground-penetrating radar (GPR): Field experiment. Near Surface Geophysics, 12, 777-791.

Słowik, M., 2014b. Holocene evolution of meander bends in lowland river valley formed in complex geological conditions (the Obra river, Poland). Geografiska Annaler: Series A, Physical Geography, 96(1), 61-81.

Słowik, M., 2015. Is history of rivers important in restoration projects? The example of human impact on a lowland river valley (the Obra River, Poland). Geomorphology, 251, pp.50-63.

Słowik, M., Dezső, J., Kovács, J., Gałka, M., Sipos, G., 2021. Phases of fluvial activity in loess landscapes: Findings from the Sió valley (Transdanubia, central Europe). Catena, 198, 105054.

Sneddon, C., Barraud, R., Germaine, M.A., 2017. Dam removals and river restoration in international perspective. Water Alternatives, 10(3), p.648.

Soar, P.J., Thorne, C.R., Downs, P.W., Copeland, R.R., 1998. Geomorphic engineering for river restoration design. In Engineering Approaches to Ecosystem Restoration, 508-513.

Szuch, R.P., White, J.G., Vepraskas, M.J., Doolittle, J.A., 2006. Application of ground penetrating radar to aid restoration planning for a drained Carolina bay. Wetlands, 26(1), 205-216.

Thiel, C., Buylaert, J.P., Murray, A., Terhorst, B., Hofer, I., Tsukamoto, S., Frechen, M., 2011. Luminescence dating of the Stratzing loess profile (Austria)–Testing the potential of an elevated temperature post-IR IRSL protocol. Quaternary International, 234(1-2), 23-31.

Thompson, D.M., Stull, G.N., 2002. The development and historic use of habitat structures in channel restoration in the United States: The grand experiment in fisheries management, Geogr. Phys. Quaternaries, 56, 45–60.

Thompson, W.K., Christensen, J., Murray, A.S. and Autzen, M., 2024. Direct dating of an ancient stone causeway at Karlslunde, Sjælland, Denmark: A combined approach using luminescence from the surfaces of granitic cobbles and coarse grains from disaggregated heated rocks. Quaternary Geochronology, 82, p.101549.

Tipping, R., 1995. Holocene evolution of a lowland Scottish landscape: Kirkpatrick Fleming Part III, fluvial history. The Holocene, 5, 184–195.

Tipping, R., Milburn, P., Halliday, S.P., 1999. Fluvial processes, land-use and climate change 2000 years ago in upper Annanndale, southern Scotland. In: Brown, A.G., Quine, T. (Eds.), Fluvial Processes and Environmental Change. Wiley, Chichester, pp. 311–328.

Tockner, K., Schiemer, F., Baumgartner, C., Kum, G., Weigand, E., Zweimuller, I., Ward, J.V., (1999), The Danube restoration project: Species diversity patterns across connectivity gradients in the floodplain system, Reg. Rivers Res. Manage., 15, 245–258.

Van Cleef, J.S., 1885. How to restore our trout streams, Trans. Am. Fish. Soc., 14, 50–55.

Vandenberghe, J., van Overmeeren, R.A., 1999. Ground penetrating radar images of selected fluvial deposits in the Netherlands. Sedimentary Geology, 128(3), 245-270.

Wallinga, J., 2002. Optically stimulated luminescence dating of fluvial deposits: a review. Boreas, 31(4), 303-322.

Walker, J., Gibson, J., Brown, D., 2007. Selecting fluvial geomorphological methods for river management including catchment scale restoration within the environment agency of England and Wales. International Journal of River Basin Management, 5(2), pp.131-141.

Weckwerth, P., Przegiętka, K., Chruścińska, A., Pisarska-Jamroży, M., 2013. The relation between optical bleaching and sedimentological features of fluvial deposits in the Toruń Basin (Poland). Geological Quarterly, 57(1), 31-44.

Wightman, S., Schofield, L., 2021. Case study 23. Swindale Valley, Haweswater, Environment Agency.

Wilby, R.L., Beven, K.J., Reynard, N.S., 2008. Climate change and fluvial flood risk in the UK: more of the same? Hydrological Processes, 22(14), 2511-2523.

Wild, C., Wells, C., Anderson, D., Boardman, J., Parker, A., 2001. Evidence for Medieval clearance in the Seathwaite Valley. Cumbria Transactions of the Cumberland and Westmorland Antiquarian and Archaeological Society, 1, 54–68.

Williams, R.D., Tooth, S., Gibson, M., 2017. The sky is the limit: reconstructing physical geography from an aerial perspective. Journal of Geography in Higher Education, 41(1), 134-146.

Williams, R.D., Bangen, S., Gillies, E., Kramer, N., Moir, H., Wheaton, J., 2020. Let the river erode! Enabling lateral migration increases geomorphic unit diversity. Science of The Total Environment, 136817.

Wilson, P., Clark, R., 1998. Characteristics and implications of some Loch Lomond Stadial moraine ridges and later landforms, eastern Lake District, northern England. Geological Journal, 33(2), 73-87.

Winchester, A.J.L., 1987. Landscape and Society in Medieval Cumbria. J. Donald Ltd, Edinburgh, p. 177.

Wohl, E., Angermeier, P.L., Bledsoe, B., Kondolf, G.M., MacDonnell, L., Merritt, D.M., Palmer, M.A., Poff, N.L., Tarboton, D., 2005. River restoration. Water Resources Research, 41(10).

Wohl, E., Lane, S.N., Wilcox, A.C., 2015. The science and practice of river restoration. Water Resources Research, 51(8), 5974-5997.

Wooldridge, C.L., Hickin, E.J., 2005. Radar Architecture and Evolution of Channel Bars in Wandering Gravel-Bed Rivers: Fraser and Squamish Rivers, British Columbia, Canada. Journal of Sedimentary Research, 75(5), 844-860.